NAVAL SHIP RESEARCH AND DEVELOPMENT CENTER
Washington, D.C. 20007

ROLL DAMPING OF CIRCULAR CYLINDERS WITH AND WITHOUT APPENDAGES

by
Alvin Gersten

HYDROMECHANICS LABORATORY
RESEARCH AND DEVELOPMENT REPORT

October 1969

Report 2621

ROLL DAMPING OF CIRCULAR CYLINDERS WITH AND WITHOUT APPENDAGES
Report 2621

The Naval Ship Research and Development Center is a U.S. Navy center for laboratory effort directed at achieving improved sea and air vehicles. It was formed in March 1967 by merging the David Taylor Model Basin at Carderock, Maryland and the Marine Engineering Laboratory at Annapolis, Maryland. The Mine Defense Laboratory, Panama City, Florida became part of the Center in November 1967.

Naval Ship Research and Development Center
Washington, D.C. 20007

NDW-NSRDC 3960/43 (10-67)

DEPARTMENT OF THE NAVY
NAVAL SHIP RESEARCH AND DEVELOPMENT CENTER
WASHINGTON, D. C. 20007

ROLL DAMPING OF CIRCULAR CYLINDERS WITH AND WITHOUT APPENDAGES

by

Alvin Gersten

October 1969 Report 2621

TABLE OF CONTENTS

LIST OF FIGURES

LIST OF TABLES

NOTATION

A	Total projected area of both appendages
b	Coefficient for "square-law" damping
c_f	Frictional resistance coefficient
E_{vib}	Total vibrational energy of system
ΔE	Energy loss per cycle
$\overline{GM}$	Metacentric height
g	Acceleration due to gravity
I	Moment of inertia about G_L of cylinder in air
$\overline{KG}$	Distance from lowest point of floating cylinder to center of gravity
k	Restoring moment coefficient
L	Length of cylinder
n	Half-cycle number
R	Radius of cylinder
R_N	Reynolds number
S	Area of cylinder wetted surface
T	Natural period
t	Time
β	Contact angle
$\tilde{\beta}$	$(\kappa/R)^2$ where κ is the radius of gyration
δ	Log decrement
ν	Fluid kinematic viscosity
ρ	Fluid mass density
ρ_B	Cylinder mass density
ϕ	Roll amplitude
ϕ_m	Mean roll amplitude, see Equation [4]
ϕ_o	Initial roll amplitude
$\dot{\phi}$	Angular velocity in roll
ω	Circular frequency = $2\pi/T$

Subscripts:

B	Due to bearings
ST	Due to surface tension
V	Due to viscosity
WM	Due to wavemaking

ABSTRACT

A research program established to provide scaling laws for roll damping involves testing five circular cylinders ranging from 3 in. to 4 ft in diameter. This report presents the results of experiments conducted on the fourth cylinder in the series, which has a 2-ft diameter and which, like those tested before it, was oscillated freely at zero forward speed. The experiments were carried out with the cylinder suspended vertically in the water both with and without appendages, and with the bare cylinder floating horizontally. In this way, the various components of damping can be isolated. Log decrements and energy loss per cycle for the bare cylinder, as well as energy loss and moment coefficients for the appendaged cylinder, are presented herein.

The results obtained thus far in the program indicate that reasonably good methods of predicting the viscous damping of different size models are available. At the conclusion of experiments with the largest cylinder in the series, sufficient information should be available for the development of an empirical equation for eddy-making damping; however, since the waves generated by the cylinder are extremely small, and therefore difficult to measure, it may not be possible to separate the contribution of wave-making damping from that of surface tension by means of the test methods presently employed.

ADMINISTRATIVE INFORMATION

The study reported herein was performed at the request of the Naval Ship Engineering Center under Task 1711 of Project No. S-F013 02 03. The request was made in Naval Ship Engineering Center letter Serial 442-047 of 13 August 1964.

INTRODUCTION

There exists a lack of information on the methods of predicting ship roll response in waves from measurements made on a dynamically scaled model. The need for scaling laws was clearly demonstrated when two models of the same submarine were tested at the Davidson Laboratory of the Stevens Institute of Technology (DL), and the Naval Ship Research and Development Center (NSRDC). The DL model was 1/80 scale and the NSRDC model was 1/25 scale. When the roll behavior of the models at zero forward speed in similar, scaled waves was compared, it was found that the rolling motions

of the larger model were approximately twice those of the smaller one. In addition, for both the surfaced and submerged conditions, the roll damping of the larger model was approximately one-third that of the smaller one.

Clearly, scale effects exist. Accurate prediction of full-scale rolling motions is, to a great extent, dependent upon an understanding of how the forces acting on the vessel vary as the gamut is run from small model to prototype. On a freely oscillating body, the forces are usually subdivided into those of inertia, restoration, and damping. The inertial forces are generally scaled by adjusting the moment of inertia and frequency of oscillation of the model according to Froude's Law of Comparison. The restoring force of a surface vessel is scaled to model size by decreasing the $\overline{GM}$ and displacement in conformance with the same law. The validity of this procedure will not be examined here. Rather, effort will be concentrated on an investigation of damping forces and the way they vary with model size.

The damping forces acting on a body oscillating in a fluid may be of several types, each following a different scaling law, and each being proportional to different powers of the velocity. The different kinds of forces are due to

(a) frictional (viscous) resistance,

(b) surface tension,

(c) wave making,

(d) eddy making, and

(e) internal energy dissipation (e.g., by large fluid-filled tanks).

Clearly, all of these components may not be present. If, for example, a deeply submerged vessel contained no fluid-filled tanks, neither items (b), (c), nor (e) would be acting.

Several experimental investigations have been conducted with both ship forms and cylinders to clarify the mechanism of these various energy dissipators. Among these is the work done by Kato[1,2] on viscous damping and Ueno[3] on surface tension damping. More recently, Ochi[4] presented the

---

[1]References are listed on page 55.

status of knowledge on roll behavior, and recommended further studies which should be conducted. His recommendations led to the establishment of a research program designed to investigate the damping of circular cylinders ranging from 3 in. to 4 ft in diameter. This program was financially supported by the U.S. Navy and the work was performed initially at DL and then at NSRDC.

The Davidson Laboratory has completed testing of the smaller cylinders.[5,6] This paper presents results obtained on the 2-ft diameter cylinder at NSRDC. The tests were carried out

(a) with the bare or appendaged cylinder mounted so that its longitudinal axis was vertical.

(b) with the bare cylinder freely floating horizontally at a draft of 80 percent of its diameter.

The viscous and eddy-making damping forces could be isolated for study by means of the type (a) tests since, when the cylinder is bare, only viscous nonconservative forces are significant, and when appendages are installed, both viscous and eddy-making forces are extant. During the type (b) tests, energy losses due to surface tension and wavemaking occur in addition to those attributable to viscous shearing stress. The present writer has utilized some of the results which were presented in Reference 5 in the form of log decrements, but has modified their form to energy losses. This was done so that a comparison between measured and predicted energy losses due to viscous effects could be made over a wide range of Reynolds numbers. Since a 4-ft-diameter cylinder will be tested at NSRDC in the future, no attempt is made in this report to derive final conclusions based on the data obtained to date. This will be done when all the experimental work has been completed. However, in order to maintain continuity with the work carried out at DL, both their experimental method and method of analysis have been adhered to wherever possible. Supplementary analyses of the data obtained with the bare cylinders have been performed in order to clarify several points.

DESCRIPTION OF MODEL AND APPENDAGES

The model used for these experiments is a circular cylinder, 2 ft in diameter and 8 ft 1/2 in. long. It was fabricated from 6061-T6 aluminum. The outside surface was machined to a smooth finish and Amchem "Alumiprep" and zinc chromate primer were applied to prevent corrosion. Several coats of DuPont "Preparakote," an alkyd-resin paint primer, were then sprayed on, with each coat wet-sanded, so that an extremely smooth surface resulted. The primer was used as the final surface since previous experience with an enamel outer coat showed that many small bump-like irregularities would develop in the enamel after prolonged immersion in the basin water. The DL models[5] had been manufactured from lucite. This material was not used in the NSRDC model because of the difficulty of fabricating a large cylinder from lucite, and because of the danger of large cracks developing during rigging operations. The inside of the cylinder was provided with bulkheads having many holes in them. Ballasting rods could be moved from one set of holes to another to provide a desired radial mass distribution. The model dimensions and dynamic characteristics were Froude-scaled from those of the 12-in.-diameter cylinder tested at DL. The particulars of the model for both the vertical and freely floating test conditions are presented in Table 1.

The moment of inertia I was established at its proper value in several steps. First, the unballasted model was suspended from the torsion rod and allowed to oscillate freely in air about its longitudinal axis. Its moment of inertia was computed from $I = (T/2\pi)^2 k$ where T is the measured period of oscillation and k is the "spring constant" of the torsion rod. The distribution of the ballast rods required to yield the proper I value for the tests with the cylinder vertical was then calculated, and the final I value for the ballasted cylinder was checked by a second free oscillation of the cylinder. Prior to testing with the cylinder floating, an inclining experiment was conducted so that the proper transverse $\overline{GM}$* was established. The ballast rods were then adjusted,

---

*For a circular cylinder, the metacenter is located at the geometric center. Thus, $\overline{GM} \equiv \overline{GO}$, where O is the centroid of the circular cross section.

without disturbing the center of gravity of the model, so that the scaled roll period was obtained. This yielded the proper moment of inertia and restoring moment coefficient.

The bilge keel and streamlined fin appendages used during two phases of the test program are shown mounted on the model in Figure 1. Although not shown in the sketch, two appendages of the same type were mounted diametrically opposed so that the side force acting on the cylinder would be cancelled out.

TEST SETUP AND INSTRUMENTATION

MODEL SUSPENDED VERTICALLY

The experiments were conducted near the center of the Rotating Arm Basin, which is a circular tank 260 ft in diameter and 21 ft deep. The tests in air were performed in a drydock which can be moved on tracks to almost the center of the basin.

During the tests with the cylinder mounted vertically, a 62 $\frac{1}{2}$ in. long by 5/8 in. diameter beryllium copper torsion rod was used to support the model and provide the restoring moment for damped oscillation about the longitudinal axis of the cylinder. The model and torsion spring assembly was mounted on a frame, the latter being fixed to the rotating arm carriage as shown in Figure 2. The frame not only supports the model via the torsion rod, but also contains two sets of bearings (one near the lower end of the torsion rod, and the other below the lower end of the model) which restrain sideward translation of the cylinder. The model was ballasted to a weight slightly greater than its displacement so that the torsion rod was always in tension and would not bow.

The couple needed to rotate the model to its initial angular displacement was provided by a cable passing around two bolts on top of the model, and thence to a system of pulleys which permitted the hanging of weights at the end of the cable. The model was released impulsively by burning a nylon bridle that spanned the distance between the aforementioned bolts. In order to minimize end effects the cylinder was situated with its upper end 0.5 in. out of the water.

A voltage proportional to angular displacement of the cylinder was obtained in two ways: (a) by strain gaging the upper part of the torsion spring and (b) by utilizing gears to turn the shaft of a rotary differential transformer. Since the latter method suffered from zero drift due to slippage of the gear mounted on the transformer, only records obtained from the former method were analyzed. The pointer and protractor shown in Figure 2 were used for calibrating the transducers.

When the bilge keel appendages were installed, a 1-ft-long section of one keel was mounted on the flexure shown in Figure 3a, and separated from the remainder of the keel by a 0.01-in. gap. The flexure was strain gaged so that with proper electronic instrumentation, a voltage proportional to bending moment existing at the strain-gage location could be obtained. Rather than measuring the strain in the flexure at two locations in the radial direction (which was difficult with so narrow an appendage) and thus precisely determining where the resultant force acted on the keel, it was arbitrarily assumed that the center of force was at the mid-depth of the keel. This is reasonable since a small difference between the actual and assumed center of force would result in a negligible error in the computed moment acting about the centerline of the cylinder. This moment acting about the centerline of the cylinder is the damping moment which is sought. Two sets of strain gages were, however, fixed along the length of the flexure-mounted section. The output of the two electronic bridges which these gages were part of, was summed to yield the average bending moment at the two locations.

The experiments with the streamlined fins were conducted with one entire fin flexure mounted (see Figure 3b) and the flexure strain gaged so that both the location and magnitude of the resultant force on the fin could be determined. With this information the damping moment could be calculated.

The transducer signals were amplified and recorded on a strip chart recorder. A sample of the records made during tests with the appendages installed is presented in Figure 4.

MODEL FLOATING HORIZONTALLY

When the bare cylinder was tested in the floating condition, the test setup shown in Figure 5 was utilized. A rod with two pins on it was attached to one end of the model so that a heeling couple could be applied by running a cable around the pins. The system was analogous to that used with the model vertical and, as before, the cylinder was released from its displaced position by burning a piece of nylon line between the pins. Since the model was completely unrestrained for these tests, some sway and heave motions could have occurred as it oscillated in roll. These motions would be expected because the center of gravity of the cylinder was below its static roll axis (the centerline), and a transverse centrifugal force would exist. Since a couple was applied to heel the model over, it drifted very little during a test.

Oscillation of a semisubmerged circular cylinder about its longitudinal axis should result in the generation of extremely small waves,[7] and it was expected that the somewhat larger waves produced by a cylinder floating at a draft of 80 percent of its diameter could still not be resolved with the wave measuring apparatus available at NSRDC. However, it was thought that the sideward motions would cause a detectable, if not measurable, disturbance of the water surface. Such a disturbance was indeed detected by a 0.005-in.-diameter wire resistance probe* mounted approximately 4 ft from the side of the cylinder, but the measurements were neither repeatable nor periodic, casting doubt upon the usefulness of the records. The maximum wave heights (crest to trough) were on the order of a few hundredths of an inch.

A Minneapolis-Honeywell pitch-roll gyroscope was used as the roll transducer. Its output was amplified and recorded on a strip chart recorder.

---

*The wave probe was calibrated in intervals of 0.1 in. For this change in water level, the amplified signal was approximately 120 millivolts. A strip chart recorder of the type utilized will normally make a visible response to a signal as small as 30 millivolts which is equivalent to a water level change of 0.025 in.

TEST PROGRAM

As indicated previously, the investigation was divided into several phases so that the various components of the damping force (see Page 2) could be isolated. Since this procedure had also been followed at DL, it is expected that scaling laws for several types of damping will ultimately be derived.

The damping in air of the bare model suspended vertically from the frame was determined first so that results from subsequent tests in water could be corrected for bearing friction and internal friction in the torsion rod. Tests were then conducted with the cylinder, both bare and with the two types of appendages, suspended in water. Since the energy loss per cycle of the bare cylinder in water was quite small, the correction obtained from the tests in air was not negligible. Finally, the model was tested while floating horizontally at a draft equal to 80 percent of its diameter (i.e., 1.6 ft).

The experiments were conducted with initial angular displacements of the model ranging from approximately 12 to 40 deg so that the effect of initial angle on damping could be evaluated.

PRESENTATION AND DISCUSSION OF TEST RESULTS

BARE CYLINDER SUSPENDED VERTICALLY*

Typical amplitude decay curves for the bare cylinder oscillating freely in air are presented in Figure 6.† For all bare cylinder tests the average amplitude of the angular displacement (i.e., average of the maximum displacement clockwise and counterclockwise for a particular cycle) is plotted as a function of cycle number. When the damping was small, it was

---

*This section is limited to discussion of results obtained by examining the first fifteen cycles of oscillation so that the presentation will conform with that made by DL.[5] Analysis of the larger number of oscillations recorded will be discussed in Appendix A.

†During the "in-air" experiments, the bearing below the model was submerged in water to insure that the friction contributed by it would be the same for experiments with the model in air and in water.

not possible to use successive amplitudes for each half-cycle without averaging because a shift in the zero existed. This resulted in all of the maximum displacements in one direction being larger than those in the other direction, rather than there being a decrease in amplitude for successive half-cycles. The zero shift which is superposed on the damped oscillation appears to be a physical characteristic of such oscillations rather than being caused by the electronic instrumentation. Kestin and Persen[8] in their analytical studies of the free oscillations of an infinite circular disk have discovered that the motion is a damped harmonic oscillation about a drifting zero position.

Although data points for only one test are shown for each initial angle, at least two runs were actually made. The results repeated reasonably well considering that all log decrements δ were small; the largest difference between log decrements for the same initial angle was 0.0011, and the average difference for all initial angles was 0.0007. The damping appears to be linear if one neglects the transitory motion occurring immediately after release. It can be assumed that the damping in air is primarily due to energy losses in the bearings and that aerodynamic viscous damping is negligible. The average δ_B values (subscript B designates . . . due to bearings) obtained from the repeated runs are listed in Table 2 where it is indicated that the log decrement decreases appreciably as the initial angle increases. It is also of interest to note that in all of the bare cylinder tests, both in and out of water, the oscillations were isochronous even when the initial angle was large.

Amplitude extinction curves for the bare cylinder oscillating freely in water are presented in Figure 7. Again, several tests were conducted for each initial angle, and the values given in Table 2 are the averages obtained from these repeated tests. The largest difference between δ_{V+B} values (subscript denotes . . . due to viscosity plus bearings) for the same initial angle was 0.0058, and the average difference for all initial angles was 0.0017. The same bearing losses that occurred for the tests in air, are present during these tests. It can be seen in Table 2 that the log decrement in water is the same order of magnitude as the decrement in air, with the δ_{V+B} values tending to decrease with increasing initial angle (one relatively small, inconsistent increase in the log decrement does occur as the initial angle increases from 12 to 20 deg).

The log decrement attributable to hydrodynamic viscous effects only, can be obtained from

$$\delta_V = \delta_{V+B} - \delta_B \qquad [1]$$

This is true since, if the log decrement is small, it can be physically interpreted as the ratio of energy lost per cycle to twice the total vibrational energy of the system.[9] That is,

$$\delta = \frac{\Delta E}{2E_{vib}} \qquad [2]$$

where $E_{vib} = 1/2\ k\ \phi^2_{mean}$,

k = "spring constant" of vibratory system, and

ϕ_{mean} = mean amplitude of oscillation for cycle of interest.

Thus,

$$\delta_V = (\Delta E_{V+B} - \Delta E_B)/2E_{vib}$$

which yields Equation [1].

Values of δ_V are also presented in Table 2. In contrast to the decrements from which it was derived, the log decrement due to viscous effects generally increases as the initial angle increases when the angles are small; it then remains essentially constant for initial angles of 30 and 40 deg. The manner in which δ_V changes with initial angle in Table 2 is primarily a reflection of the way δ_B decreases rapidly (compared to δ_{V+B}) with increasing angle. Moreover, in order to obtain δ_V, it was necessary to subtract two small (experimentally obtained) values which are the same order of magnitude. It is, therefore, not possible to state unequivocally that the relationship between δ_V and initial angle is actually exactly as shown. Nevertheless, some dependence of δ_V on initial angle is clearly indicated. A paper by Cummins[10] provides one possible explanation for this dependency. He presents a form for the equations of motion of an oscillating ship, involving an integro-differential equation containing convolution integrals over the past history of the velocity. For a rolling body these integrals can be written as

$$\int_{-\infty}^{t} K_{\phi}\,(t - \tau)\,\dot{\phi}\,(\tau)\,d\,\tau$$

where $K_{\phi}(t)$ is a function of time which is independent of frequency, and

$\dot{\phi}(t)$ is the angular velocity in roll.

The component of this integral which is 90 deg out of phase with the motion contributes to the damping. Since the time history of angular velocity varies with initial angle, it is clear that the damping should also be variable.

Tanaka[11] has presented a theoretical discussion of the viscous damping of rotational oscillations of a circular cylinder in which he assumes that the flow is laminar, there is no free surface, and end effects can be neglected. His solution for the log decrement is given by

$$\tilde{\beta}\,\frac{\rho_{\tilde{B}}}{\rho} \cdot \alpha T = \sqrt{2}\,\pi\,\sqrt{\frac{R^2\,\omega}{\nu}} \qquad [3]$$

where $\tilde{\beta}$ is a coefficient depending on the distribution of mass of the cylinder = $(\kappa/R)^2$, where κ is the radius of gyration

$\rho_{\tilde{B}}$ is the density of the cylinder,

ρ is the fluid mass density,

α is the damping factor,

T is the period of oscillation,

$\alpha T \equiv \delta_V$ is the logarithmic decrement,

R is the cylinder radius,

ω is the circular frequency = $2\pi/T$, and

ν is the fluid kinematic viscosity.

The results obtained by DL with small cylinders were presented in Figure 13 of Reference 5 along with data obtained by Kato[1,2] and the theoretical prediction of Tanaka. The figure is reproduced as Figure 8 in this report, and the data obtained at NSRDC with the 2-ft-diameter cylinder (from Table 2) have also been included. The theoretical relationship between dimensionless log decrement coefficient and Reynolds number was corroborated reasonably well by both the DL and Kato results even though differences

exist in the length to diameter ratio.* The NSRDC data also tend to follow the trend suggested by the theory. However, there is, in this case, a scattering of the points above and below the theoretical line, with the largest value differing from the smallest by a factor of almost two. This, of course, is a manifestation of the apparent initial angle effect discussed earlier. In summary, the available empirical results indicate that at least for Reynolds number $R^2\ \omega/\nu$ between approximately 1.0×10^4 and 2.2×10^5, Equation [3] yields a reasonably good prediction of the log decrement due to hydrodynamic viscous effects acting on a circular cylinder. There is, however, an indication of initial angle effect which is not included in the theory.

Some of the experimental results obtained by Kato[1,2] have been presented in Figure 8. As a result of his studies with cylinders completely immersed in water, Kato obtained the following formula for the work done during one cycle by the frictional resistance associated with roll

$$\Delta E_V = \frac{16}{3}\ \rho\pi^2\ C_f \phi_m S R^3 \phi_m^2 \left(\frac{1}{T^2}\right) \qquad [4]$$

where C_f is the frictional resistance coefficient,

ϕ_m is the mean roll amplitude = $1/2\ (\phi_i + \phi_{i+1})$, ϕ_i and ϕ_{i+1} being successive positive (or negative) amplitudes of oscillation, and

S is the area of wetted surface.

Kato showed (again based on his experiments) that

$$C_f\ \phi_m = 0.74 \sqrt{\frac{T\ \nu}{R^2}} + \phi_m \frac{2.2}{10^{19}} \frac{R}{T^3 \nu^3} \qquad [5]$$

For the conditions which existed during both the DL and NSRDC tests, the second term on the right hand side of Equation [5] is extremely small.

---

*Discussion of the effect of L/D can be found in Reference 6.

Thus, Equation [4] can be written as

$$\Delta E_V = \frac{16}{3} \rho \pi^2 \left(0.74\sqrt{\frac{T\nu}{R^2}}\right) SR^3 \phi_m^2 \left(\frac{1}{T^2}\right) \qquad [6]$$

From Equation [5]

$$C_f \tilde{=} (0.74)\frac{1}{\sqrt{\frac{R^2\phi_m^2}{T\nu}}} = 1.328\frac{1}{\sqrt{\frac{3.22R^2\phi_m^2}{T\nu}}} \qquad [7]$$

The Blasius formula for the laminar flow friction coefficient is given by

$$C_f = 1.328\frac{1}{\sqrt{\frac{vL}{\nu}}} = 1.328\frac{1}{\sqrt{R_N}}$$

where v is the velocity,

L is the characteristic length = const. x $R\phi_m$ for rolling motion, and

R_N is the Reynolds number.

Thus, the frictional coefficient for an oscillating cylinder can be expressed in the same form (i.e., as a function of Reynolds number) as that given by Blasius if, in Equation [7], R_N can be taken as

$$R_N = \frac{3.22R^2\phi_m^2}{T\nu}$$

Instead of using Equation [6], values of ΔE_V can be calculated from experimentally determined values of δ_V and Equation [2]. This type of calculation was made for the DL and NSRDC results and was plotted in Figure 9 along with values obtained from Equation [6].

The initial angular displacement ϕ_o was used, rather than ϕ_m, in the calculations for this graph, since the former were known for the DL tests, and ϕ_m is dependent on the cycle number arbitrarily selected. This utilization of ϕ_o will not affect the agreement between the empirical Equation [6] and the DL-NSRDC results since selection of a ϕ (or ϕ_m) < ϕ_o would merely result in a shift of the data point parallel to the predicted

line, and the percent difference between ΔE_V values at the lower value of R_N would remain the same. In Figure 9a no data points are shown for NSRDC results because all except one lie above $\Delta E_V = 0.1$. Since cylinder diameter was selected as the parameter in Figure 9, variation of Reynolds number for each line and its associated data points is due only to changes in initial angle.

Good agreement between the predicted and experimental values of ΔE_V is to be expected since, as shown in Figure 8, the related log decrements agree in magnitude and/or relationship to $R^2\ \omega/\nu$. This is indeed the case in Figure 9. Thus, Kato's equation derived from his experiments with cylinders up to 12.0 in. in diameter, is useful for predicting viscous energy loss and damping coefficients for Reynolds numbers $[3.22\ \phi^2\ (R^2/T\nu)]$ ranging from approximately 8.0×10^1 to 6.0×10^4. Although the largest cylinder tested thus far is only 24 in. in diameter, the large initial angles used resulted in fairly high Reynolds numbers which may fall in the range applicable for a full scale ship.

Figure 10 shows ΔE_V plotted as a function of R_N, with amplitude of roll as the parameter, to illustrate Kato's prediction for the change in energy lost per cycle as ϕ changes. Although the initial angles employed at DL were slightly different from those utilized at NSRDC, ΔE_V could be computed for the NSRDC values of ϕ_o since DL found δ_V to be essentially invariant with initial angle. Equation [2] was used for this purpose and the values are also plotted in Figure 10. The agreement between prediction and experiment is satisfactory.

BARE CYLINDER FLOATING HORIZONTALLY

Roll Decrement

Examples of the roll decay curves for the floating condition are presented in Figure 11 where the ordinate is the average amplitude (i.e., average of maximum displacement clockwise and counterclockwise) for the cycle designated on the abscissa. The damping is quite linear for all initial angles. This is not the case for small models. Figure 4 of Reference 5 shows that the damping of a 3-in.-diameter cylinder is highly nonlinear and that the damping gradually becomes more linear as the diameter

is increased to 6 in. and 12 in. This is an interesting scale effect which did not exist when the models were suspended vertically, in which case only viscous energy losses were significant. When the model is floating, surface tension and wave making damping components can also be present and it is either one or both of these which contribute to nonlinear damping for small models. It should be pointed out that the restoring moment was nonlinear for all the floating cylinders; this was especially true for large initial angles. Average values of $\delta_{V+ST+WM}$ (subscript denotes . . . due to viscosity, surface tension, and wave making) are presented in Table 3 which shows that the initial angle effect is quite small.

Energy Loss

The total energy loss per cycle was computed from the log decrements of Table 3 and is presented as $\Delta E_{V+ST+WM}$ in Table 4. In order to break this total energy loss down into its components, ΔE_V for the floating cylinder was calculated from ΔE_V for the vertical cylinder (see Figure 9) by reducing the latter values by the factor $\frac{\text{wetted surface floating}}{\text{wetted surface vertical}}$. These results are tabulated in column three of Table 4. The difference between $\Delta E_{V+ST+WM}$ and ΔE_V yields the energy loss due to surface tension and wavemaking (ΔE_{ST+WM}) which is also listed in the table. It was not possible quantitatively to determine the components of ΔE_{ST+WM}. As discussed previously, the waves generated by the rolling cylinder could not be measured accurately; this prevented exact evaluation of ΔE_{WM}. A rough indication of this quantity can, however, be obtained from information contained in Reference 7, and from the water disturbance which was measured, albeit imprecisely, during these experiments. Reference 7 treats theoretically the waves generated by a semi-immersed circular cylinder which is rolling about its center on the free surface of a viscous liquid. The ratio of wave amplitude to the amplitude of motion at the periphery of the cylinder is derived as*

$$\left|\frac{\tilde{A}\pm}{R\phi_o}\right| = \pm\, 4\, m^2\, R1 \qquad [8]$$

*Notation changed to conform with that utilized in this paper.

where $\tilde{A}$ is the wave amplitude,

$$m = \frac{\omega^2}{g}$$

g is the acceleration due to gravity, and

$$l = \sqrt{\frac{\nu}{\omega}}$$

Equation [8] yields a wave height of approximately 0.005 in. for oscillation of the 2-ft-diameter cylinder at an amplitude of 40 deg. The highest wave disturbance actually recorded was approximately 0.035 in. crest-to-trough, which is considerably higher (a factor of 7) than the value predicted by Equation [8]. However, the measured waves were produced, in part, by sway and heaving motions of the model so that the wave height attributable to roll would be only a part of the total. Also, a rolling cylinder submerged to 80 percent of its diameter will generate higher waves than one which is only semi-immersed, if the wavemaking due to translatory motion is the same in both cases.

The energy contained in the waves emanating from both sides of the model can easily be computed if it is assumed the waves are sinusoidal. This energy is given by

$$E_{WM} = 1/8 \; \rho \; g \; \hat{H}^2 \; \hat{A} \qquad [9]$$

where $\hat{H}$ is the wave height and $\hat{A}$ is the surface area contained in a wave 34.6 ft long between crests (2.6-sec period) and having a length along a crest equal to the model length. The lower (theoretical) value of wave height presented above yields E_{WM} = 0.0004 ft-lb while the higher (measured) wave height results in E_{WM} = 0.020 ft-lb. Even the larger of these energy values is smaller than all of the values of ΔE_{ST+WM} in Table 4; this would indicate that a significant portion of the energy is being dissipated by surface tension.

Experimental and analytical studies conducted by Ueno, and reported in Reference 3, contradict this, since they show that the contribution of surface tension to roll damping will be negligible if, as in the present case, the surface of the model has a low contact angle (i.e., is easily wet) with water. To determine the contact angle β the model surface was duplicated on small samples of aluminum which were sent to the U.S. Naval

Research Laboratory, Washington, D.C. for analysis. The analysis revealed that once the surface was wetted, the contact angle between it and basin water would remain at zero degrees. The cylinder was always wet prior to the start of a damping test. The contact angle of an acrylic plastic surface, chemically similar to the Lucite used for the DL models, was found to be 69 degrees before and after previous wetting. In contrast to the NSRDC surface, the plastic exhibited a hydrophobic character which facilitated the easy and complete removal of all visible water.

An explanation of Ueno's findings can be made with the aid of Figure 12. Figure 12a shows a rolling cylinder whose surface is not easily wetted by water. The ascending side will have a different contact angle than the descending side, and there will be a net moment due to surface tension forces, opposing the rolling motion. Figure 12b represents the case of a cylinder whose surface is easily wetted. On the side that is descending, the water particles adhere to the surface that is above the ambient water level, since it had been wetted during the preceding part of the oscillation, and the water surface is drawn up so that its form is concave up just like the ascending side. The moment due to surface tension at the descending side counterbalances the corresponding moment at the ascending side. Thus, damping due to surface tension does not arise at all. In the present case $\beta_3 \cong 0$ deg. It is apparent that the values of ΔE_{ST+WM} which were obtained by subtracting ΔE_V from $\Delta E_{V+ST+WM}$, and reported in Table 4, are higher than would be obtained by existing theories. In addition, experiments conducted by McLeod and Hsieh[12] on rolling noncircular cylinders also support the contention that ΔE_{ST+WM} should be smaller. They employed a "vibrating-needle" apparatus and measured the waves generated by a floating model having reasonably similar dimensions to the one used in the present study. For a roll amplitude of 12 deg, the wave-damping energy propagated per cycle by their cylinder was approximately 0.0006 ft-lb which is much less than the value of 0.05 ft-lb presented in Table 4 for ΔE_{ST+WM}. During the present experiments, small eddies were probably generated at the ends of the cylinder because of its heaving and swaying motion. Such eddy generation, although it was produced by the translatory motions, may have caused an energy loss in roll through cross-coupling effects. This loss would be included in ΔE_{ST+WM}. Table 5, which lists the ratio of components

of energy loss to total energy loss, indicates that for small amplitudes of oscillation, the energy loss due to the combined effects of surface tension and wavemaking (and possibly eddy generation) is a large percentage of the total. More fundamental investigations, both experimental and theoretical, are needed to establish quantitatively the significance (or insignificance) of these components, acting as independent agents.

CYLINDER WITH APPENDAGES INSTALLED SUSPENDED VERTICALLY

Bilge Keels

A typical motion extinction curve for the freely oscillating cylinder with bilge keels installed (as in Figure 1a) is presented in Figure 13. Since the decrement in oscillation during the initial cycles is large, the effect of any zero shift that may exist is insignificant, and it was not necessary to average clockwise and counterclockwise amplitudes, as was done for the bare cylinder. The damping is obviously highly nonlinear; similar curves were obtained for the smaller initial angles.

Once appendages have been added to the model, most of the energy loss during an oscillation is due to the damping forces (primarily due to the generation of eddies) acting on these appendages. This has been demonstrated by the experiments of Gawn[13] which show that the contribution of hull surface roughness to the total damping of a ship model with bilge keels is quite small. Inertial forces also act on the appendages, but these are conservative and do not result in the dissipation of energy. The experiments of Brown[14] revealed that the force directly proportional to velocity (linear damping) acting on a flat plate oscillating normal to its plane was less than 10 percent of the total drag force for the amplitudes that occurred during the first ten cycles of his tests, and had no perceptible effect on the decay of the first ten oscillations. Since the initial displacement of the bilge keels was always larger in the present study, the linear damping force due to the keels mounted on the cylinder should be negligible. To check this, a plot of the decrease in amplitude per period against the mean amplitude was made on log-log paper and is presented in Figure 14. Most of the points tend to fall on a straight line. Those that do not, represent values of $- d\phi/dN$ occurring immediately after

the sudden release of the cylinder, and probably represent a transitory motion. The data points falling along the line can be represented by an equation of the form

$$- d\phi/dN = 0.11\ \phi_m^2$$

which shows that quadratic damping predominates.[5] Therefore, the total damping force proportional to the first power of velocity resulting from both skin friction* and keel action will be neglected and the equation of motion will be written as

$$I_{virtual}\ \ddot{\phi} + b\ \dot{\phi}|\dot{\phi}| + k\ \phi = 0 \qquad [10]^{\dagger}$$

Minorsky[15] has given as an approximate solution to Equation [10]

$$\phi = a(t)\ \cos\ \omega t \qquad [11]$$

where

$$\frac{1}{a} - \frac{1}{a_o} = \frac{4b\ \omega^2}{3k}\ n \qquad [12]$$

where a_o is the initial displacement,
b is the damping coefficient,
k is the restoring moment coefficient,
n is the half-cycle number = $2t/T$,
t is time, and
$I_{virtual}$ is the virtual mass moment of inertia.

Brown[14] has presented the exact solution to Equation [10] and he shows that the maximum difference between the exact and approximate solutions

---

*The force due to skin friction has been shown in a previous section of this report to be essentially linear in toto.

†Comparisons between actual motion time history and actual energy loss and those computed from Equation [10] are made in Appendix B.

is less than one-half of one percent. Therefore, Equation [12] which represents a linear relationship between 1/a and the cumulative number of half-cycles of oscillation will be used in the present analysis.

Figure 15 is a plot of $1/\phi$ versus half-cycle number; it was obtained from the data points of Figure 13. The points fall in essentially a straight line once the first few half-cycles have been completed. This tends to support the applicability of Equation [12]. Although Figure 15 is representative of most of the graphs obtained from repeated tests at various initial angles, several of the plots were somewhat more nonlinear. From the slope of each of the lines similar to that in Figure 15, the damping coefficient b was computed by means of Equation [12].* Then, in keeping with the procedure followed in Reference 5, two types of moment coefficients were computed. The first can be used to compare the effectiveness of different types of appendages in quenching roll motion. The denominator is kept constant and does not involve characteristics of the appendage. It is given by

$$\bar{C}_m = \frac{\text{damping moment}}{(\rho/2)\ \dot{\phi}^2\ \nabla^{5/3}} = \frac{b}{(\rho/2)\ \nabla^{5/3}} \qquad [13]$$

where ∇ is the immersed volume of the cylinder without appendages. The second coefficient is more useful if one is interested in scaling the moment produced by an appendage. It contains physical characteristics of the appendage and is given by

$$C_m = \frac{\text{damping moment}}{(\rho/2)\ A\ R_{c.a.}^3\ \dot{\phi}^2} = \frac{b}{(\rho/2)\ A\ R_{c.a.}^3} \qquad [14]$$

where A is the projected area of both appendages (i.e., twice that of one appendage), and

$R_{c.a.}$ is the radius from longitudinal axis of cylinder to centroid of appendage.

---

*This coefficient includes the effect of bearing friction which can be assumed small compared to the contribution of the appendages.

Values of $\bar{C}_m$ and C_m are given in Table 6, along with several geometric characteristics of the model and appendages, the period of oscillation and the ratio of virtual mass moment of inertia to cylinder mass moment of inertia. The latter was determined from

$$I_{virtual} = I + I_a = \left(\frac{T}{2\pi}\right)^2 k \qquad [15]$$

where I is the moment of inertia of the cylinder with appendages in air, about its longitudinal axis, and I_a is the fluid added-mass moment of inertia. The small effect of damping on the period of oscillation is neglected in this equation. Furthermore, the period of oscillation was not isochronous for the first few cycles; it would decrease on the order of one to two tenths of a second and then remain constant for subsequent cycles.

The strain signal obtained from the flexure-mounted bilge keel section was small (see Figure 4a) since the flexure had been designed for greater forces than it actually was subjected to (maximum loads on the 12-in. long section were on the order of 1.5 lb). The design of the flexure was based on load predictions made from information contained in the papers by Keulegan and Carpenter[16] and Ridjanovic.[17]

The energy dissipated by the keels during one cycle was computed by integrating the moments due to these measured forces as follows

$$\Delta E_{APPENDAGE} = \oint M \, d\phi \qquad [16]$$

It is of interest to compare the results obtained from the above procedure with the decrease in potential energy stored in the torsion rod during the same cycle, since the latter represents the total energy dissipated. The loss in potential energy was calculated from

$$\Delta P.E. = 1/2 \; k \left\{ \left[\phi^2_{t_o} - \phi^2_{t_{o+T}} \right]_{APPENDAGES} - \left[\phi^2_{t_o} - \phi^2_{t_{o+T}} \right]_B \right\} \qquad [17]$$

where ϕ_{t_o} and $\phi_{t_{o+T}}$ are the maximum angular displacements at the start and end of the cycle. Values of ϕ for the first term in brackets on the

right-hand side of the equation were obtained from records made during the tests in water with appendages, while those for the second term (which represents a correction for bearing losses) were obtained from records made during tests in air without appendages. In Table 7 comparison is made of the various types of energy loss occurring during a cycle, exclusive of bearing losses. The energy dissipated by frictional resistance was derived by reading ΔE_V from Figure 9b for the appropriate angular displacement and multiplying this energy loss by the ratio of average angular velocity for the cylinder with keels to that of the bare cylinder. Values of $\overline{\dot{\phi}}$ for the cycle of interest were computed from the solution of Equation [10] for the "with appendages" case and the well-known solution of the linear differential equation for the "bare" case.

The column labeled residual energy was obtained by subtracting the sum of columns 3 and 4 from column 2. It represents the accumulation of experimental and analytical errors. For example, the assumption was made that the same wetted surface exists on both the appendaged and bare cylinders. Certainly, the wake behind the appendage will affect the amount of cylinder surface wetted and the nature of the flow. In addition, a shift in the zero on the strip chart of only 1 deg can result in a residual energy which is the order of a few percent of ΔE_{TOTAL}. For the tests conducted with the bilge keels the residual energy is quite small. As expected, the energy consumed by skin friction is also very small compared to the keel work.

Streamlined Fins

The methods of data analysis and presentation for the streamlined fin configuration are similar to those employed in the previous section. The typical motion extinction curve shown in Figure 13 is highly nonlinear. It is interesting to note that although the rate of decay is initially greater for the streamlined fin than for the bilge keels, this situation is subsequently reversed so that the cylinder with bilge keels eventually has a smaller amplitude of oscillation. This same characteristic was mentioned in Reference 5.

To determine whether quadratic damping can be assumed for the fin configuration as it was for the bilge keel condition, a plot of $-d\phi/dN$

against ϕ_m was made and is presented in Figure 16. The data points all fall along a straight line which is given by the equation

$$-d\phi/dN = 0.059\ \phi_m^2$$

Therefore, damping proportional to the square of velocity predominates and the motion can be described by Equation [10]. Different inertial and damping coefficients must, of course, be used for the bilge keel and fin configurations. A representative plot of the inverse of the oscillation amplitude versus half-cycle number is presented in Figure 15 and, it too is reasonably linear. The moment coefficients $\bar{C}_m$ and C_m have been calculated, and are tabulated in Table 6 as are the natural period and virtual moment of inertia to cylinder moment of inertia ratio. The moment of inertia of the water entrained by the fin is quite large, being slightly greater than that of the cylinder itself.

The phase between the angular motion of the cylinder and the moment generated by the fins was obtained from the strip chart records. It was found to vary only slightly from one cycle to the next; the average values are presented in Table 8. The sketch accompanying the table shows how this phase angle ε is defined. It also depicts, in analogy to the forced oscillation case, a division of the total moment into damping and inertial components, the former being defined as 90 deg out of phase with the motion and the latter as 180 deg out of phase with the motion. Actually, in free oscillation with damping, the damping and inertial moments do not generally adhere to these phase relationships, but they are employed here for convenience.

A breakdown of the energy dissipated during one cycle of motion is made in Table 9. In this case, ΔE_V was obtained by multiplying values from Figure 9b by the ratio of average angular velocity for the cylinder with fins to that of the bare cylinder. The residual energy is much larger than for the tests with bilge keels. This may be due, in part, to the fact that the inertial component of the total force measured on the fins is much larger than the damping force. Integration of the moment due to the total force, as in Equation [16], should result in no energy dissipation by the inertial component (a conservative force). However, a small error in the graphical integration could result in a significant amount of net work from the inertial term, and an associated error in ΔE_{FINS}.

A plot of the moment generated by one fin versus cycle number is shown in Figure 17. The moment occurring at the instant of release, that is, at cycle number zero, is the largest one acting during a test; however, it could not be obtained from the records because of a low signal-to-noise ratio. Fortunately, the noise due to vibration of the appendage damped out rapidly.

The amplitude of the fin induced moment occurring just prior to the first maximum rotation of the model after release (cycle number 0.5) was determined from Figure 17, and decomposed into its damping and inertial components by utilizing the phase angles tabulated in Table 8. The results are given in Table 10 where it can be seen that the damping component is, at most, 25 percent of the inertial component.

CONCLUSIONS

The principal findings of this study of roll damping are presented below. The conclusions are stated with bounds on certain parameters such as size and Reynolds number because of the limits on the range of experimental verification at the present time.

1. The component of damping due to hydrodynamic viscous forces is very nearly linear (i.e., proportional to the first power of velocity). The log decrement always remains small, but does fluctuate some as many oscillations are executed.

2. The log decrement due to viscous forces acting on the 24-in.-diameter cylinder appears to depend on the initial angular displacement ϕ_o. The decrement tends to increase as ϕ_o is increased in the range of 12 to 30 deg, and then remains essentially constant as ϕ_o is increased further to 40 deg. The variation of log decrement with initial angle may be due to the fact that damping is affected by the past history of velocity, and the latter is different for different initial angles.

3. The theory of Tanaka, as represented by Equation [3] in the body of this report, yields a fairly good prediction of the roll decrement due to viscous forces for values of Reynolds number ($R^2\ \omega/\nu$) between approximately 1.0×10^4 and 2.2×10^5. The effect of ϕ_o on δ_v is not considered in this theory.

4. The energy dissipated by frictional resistance can be calculated with reasonably high accuracy by means of the empirical equation of Kato (Equation [6] in this report) for values of Reynolds number [$3.22\ \phi^2\ (R^2/T\nu)$] ranging from approximately 8.0×10^1 to 6.0×10^4.

5. When cylinders float on the free surface, in which case surface tension and wavemaking absorb energy in addition to that absorbed by viscous forces, the damping is quite linear for a 24-in.-diameter cylinder but it becomes progressively more nonlinear as diameter is decreased.

6. The log decrement of a floating cylinder is not greatly dependent on initial angle.

7. Tests on the floating 24-in.-diameter cylinder indicate that the total energy absorbed by both surface tension and wavemaking may be a significant percentage of that absorbed in toto. This cannot be substantiated by the limited studies carried out to date by other researchers on the specific subjects of wavemaking damping and surface tension damping.

8. When a rolling model has bilge keel or fin type appendages installed, its motion can be described fairly accurately by a second order differential equation containing a damping term proportional to the second power of velocity. This is because the linear damping forces contributed by skin friction and appendages are negligible compared to the quadratic damping forces associated with eddies generated by the appendages.

9. The added moment of inertia due to entrainment of water by the bilge keels is small while that due to the streamlined fins is approximately equal to the moment of inertia of the model itself.

10. If, in analogy to the forced oscillation case, it is assumed that the damping component of the moment produced by the streamlined fin acts 90 deg out of phase with the motion, and the inertial component acts 180 deg out of phase with the motion, then the former is found to be, at most, only 25 percent of the latter.

ACKNOWLEDGMENTS

The author wishes to thank Mr. R. Johnson of the Seaworthiness Branch for his assistance during the conduct of the experiments and the analysis of the data. He is also indebted to Dr. C.M. Lee for his valuable comments and suggestions. The contributions of Messrs. S.E. Callanen, G.J. Norman, R. Kenly, T. Thornburg, and E. Loncoski to the design of the various test Equipment is gratefully acknowledged.

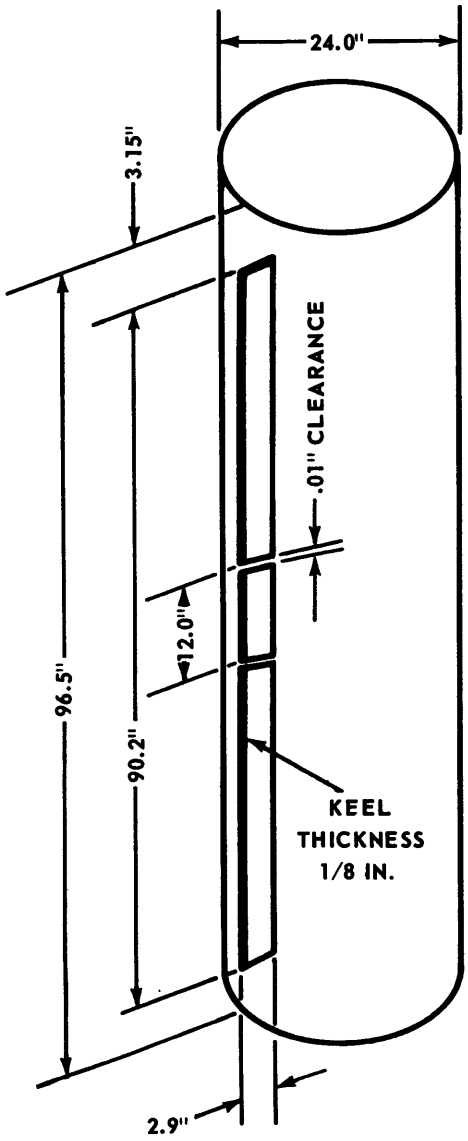

Figure 1a - Bilge Keels

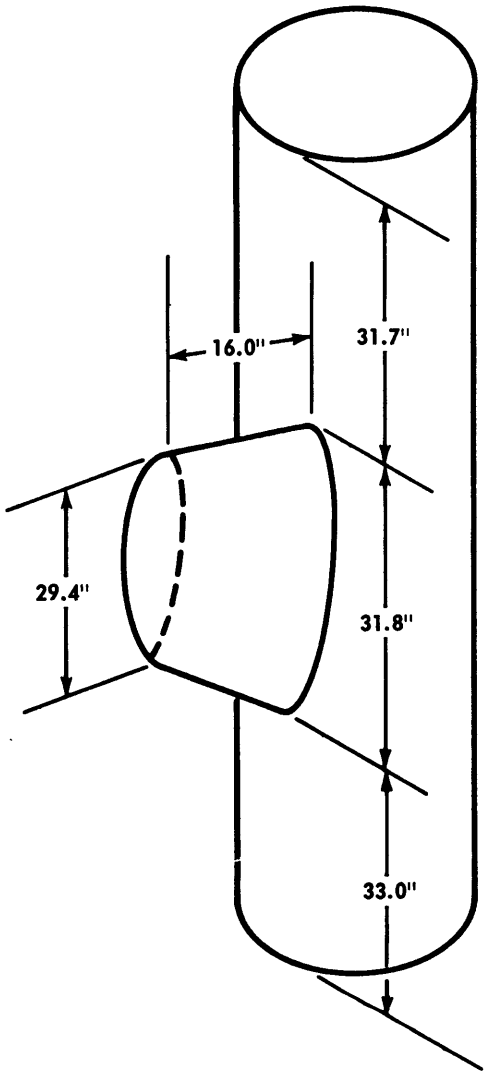

Figure 1b - Streamlined Fins

Figure 1 - 24-Inch-Diameter Cylinder with Appendages

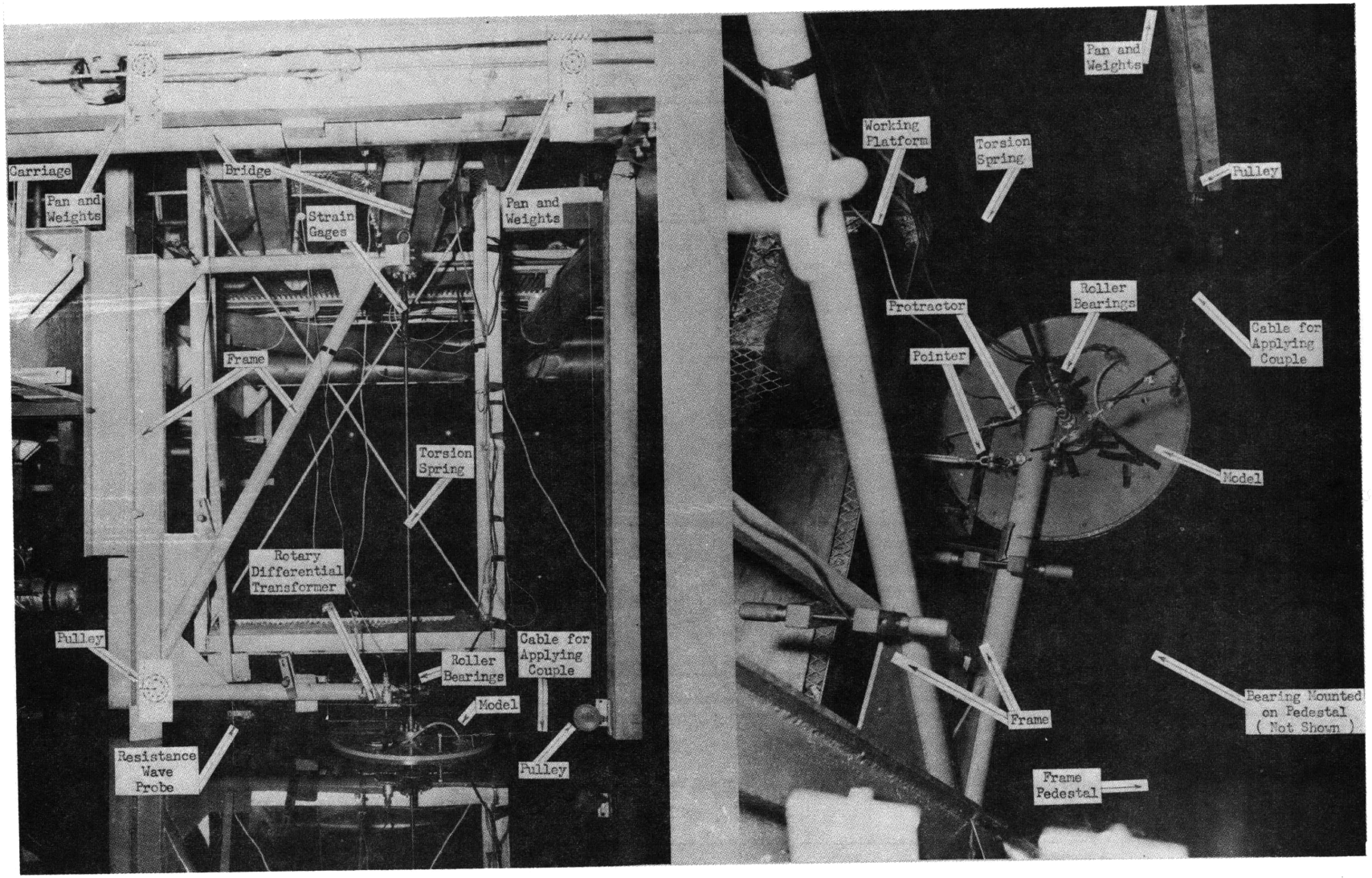

Figure 2 - Test Setup, Model Vertical

Figure 3 - Assembly of Appendages on Flexures

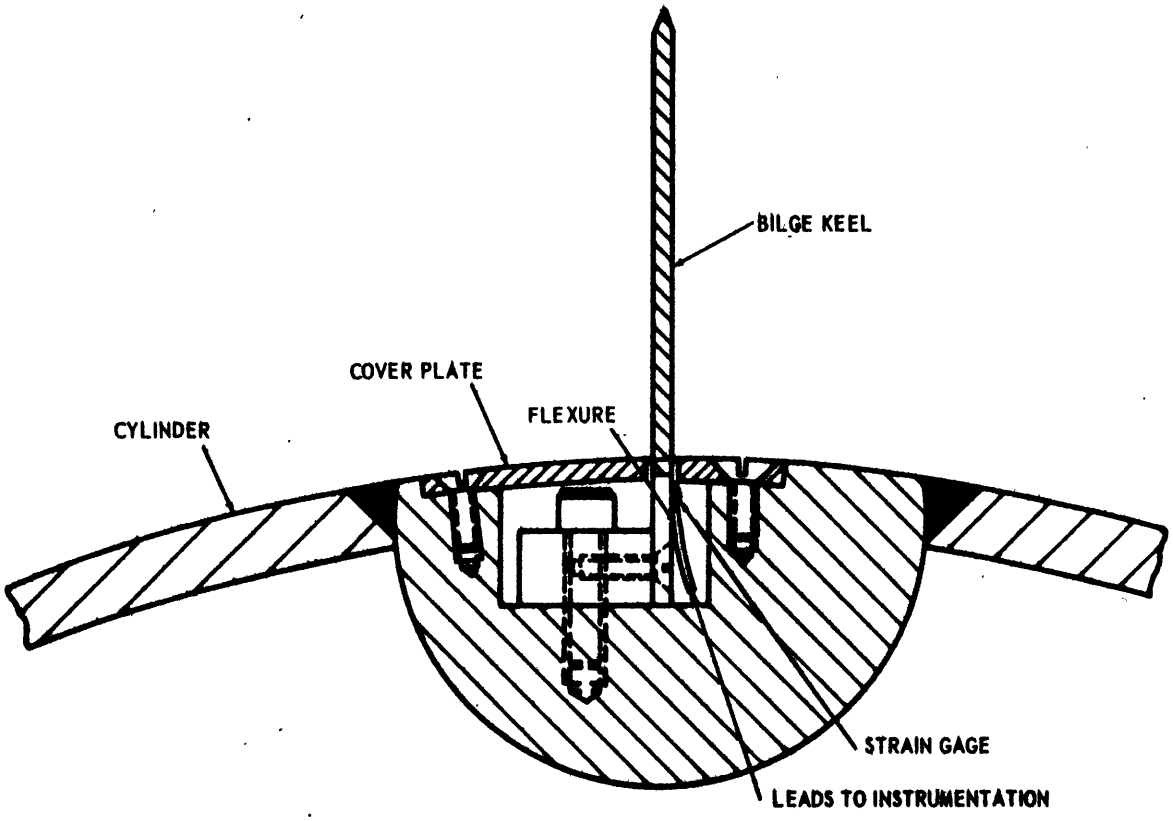

Figure 3a - Bilge Keel Assembly

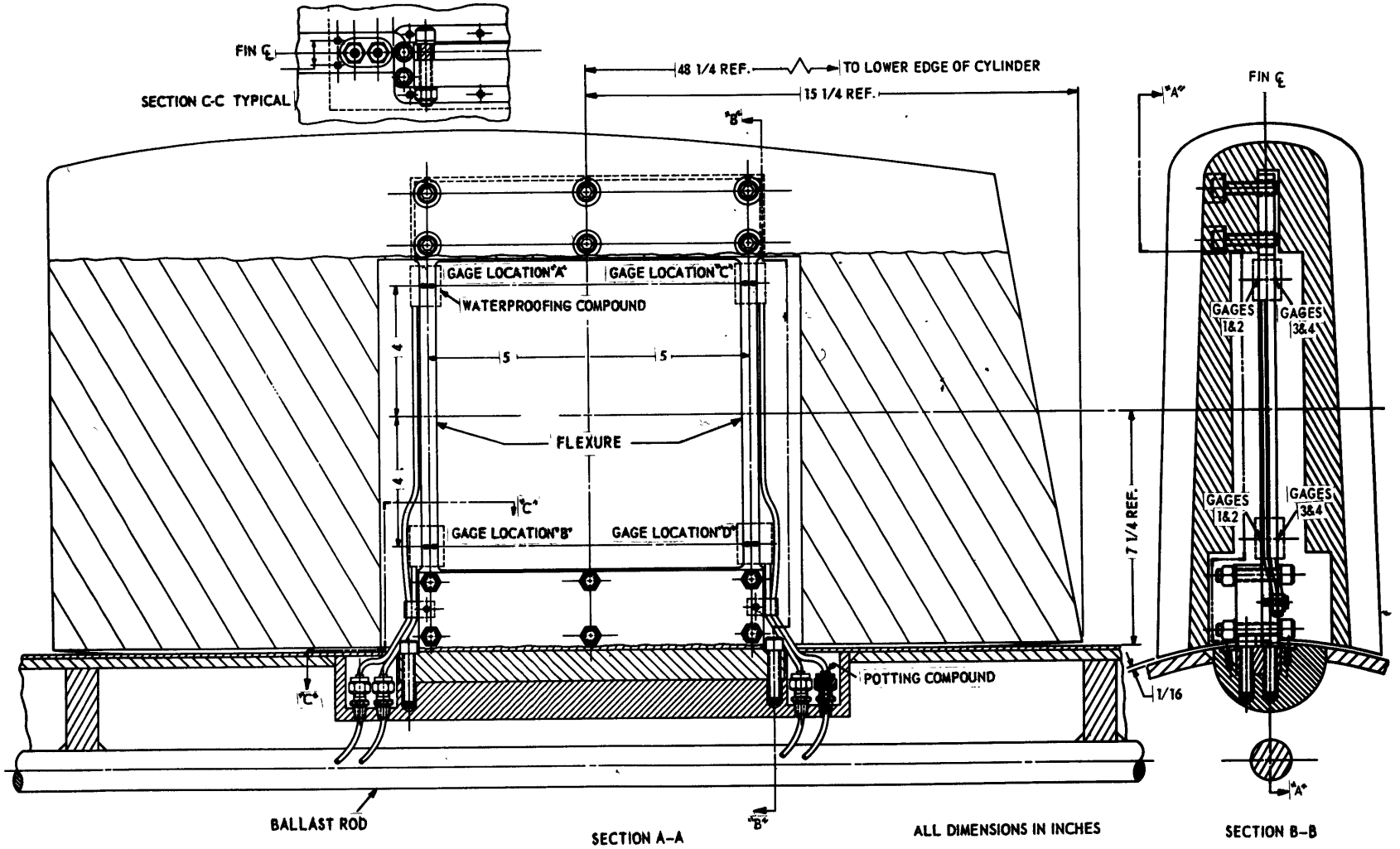

Figure 3b - Streamlined Fin Assembly

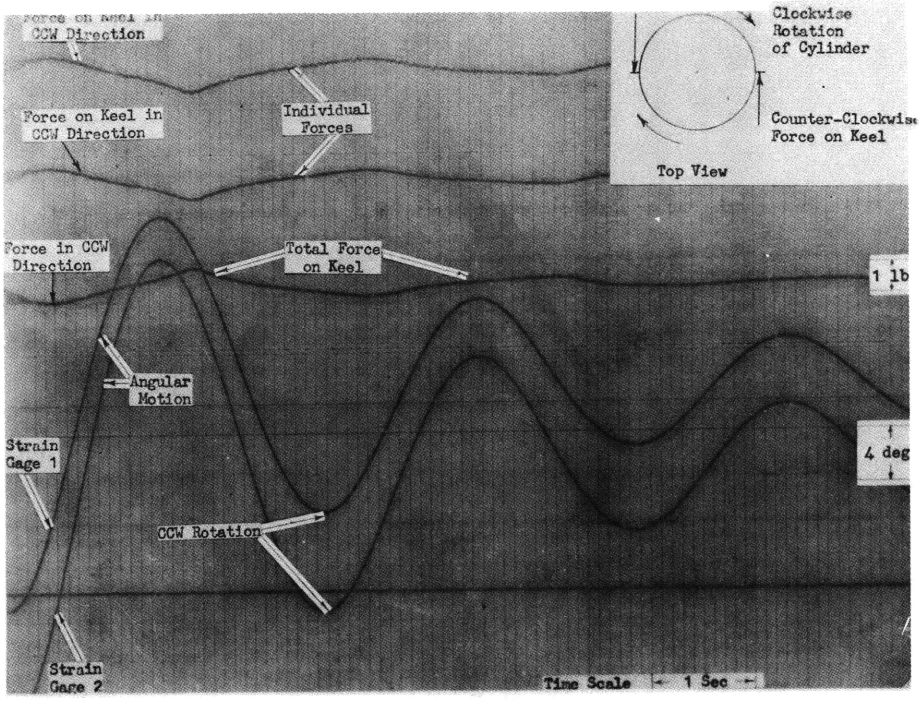

Figure 4a - Bilge Keels Installed

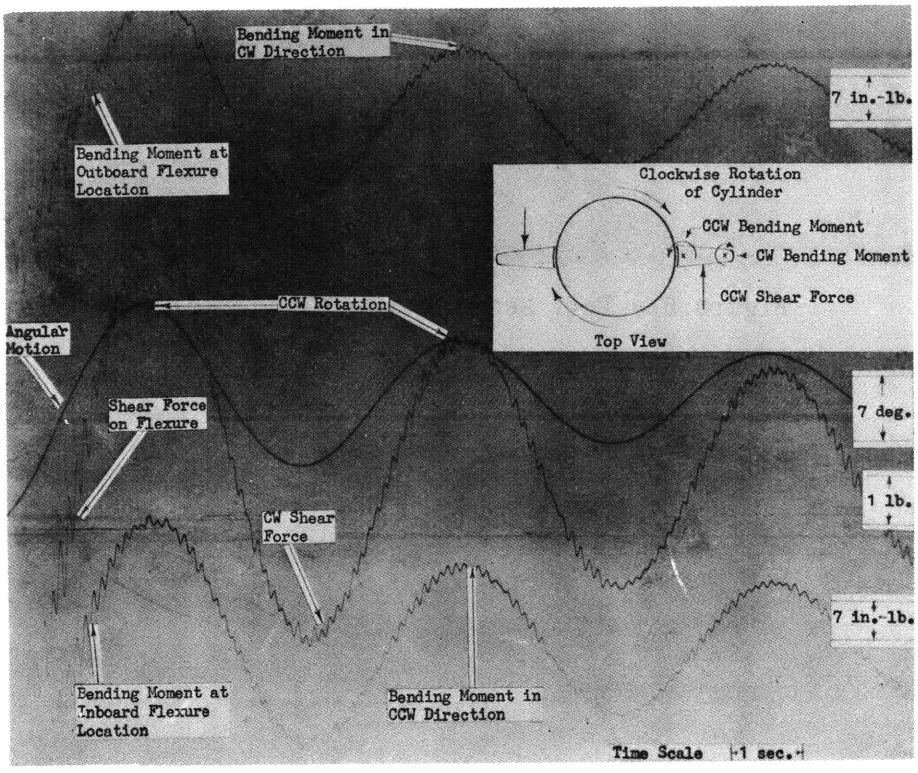

Figure 4b - Streamlined Fins Installed

Figure 4 - Sample Records

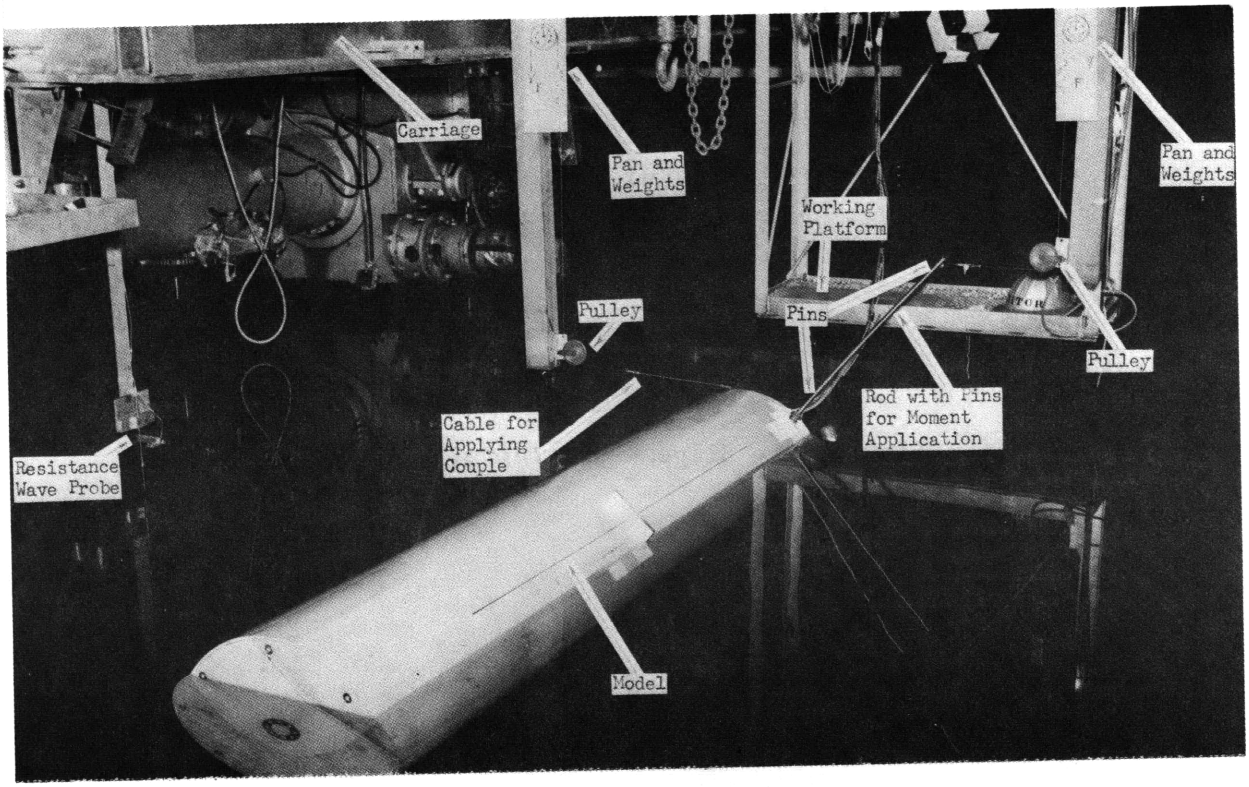

Figure 5 - Test Setup, Model Horizontal

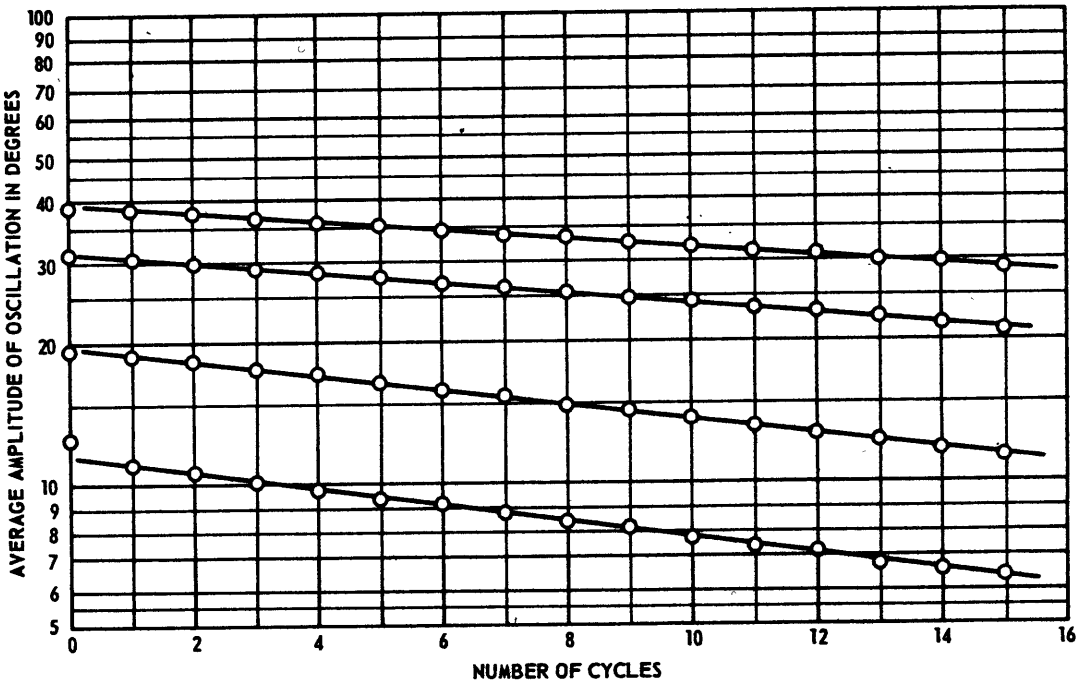

Figure 6 - Amplitude Decay of the 24-Inch-Diameter Bare Cylinder Suspended Vertically in Air

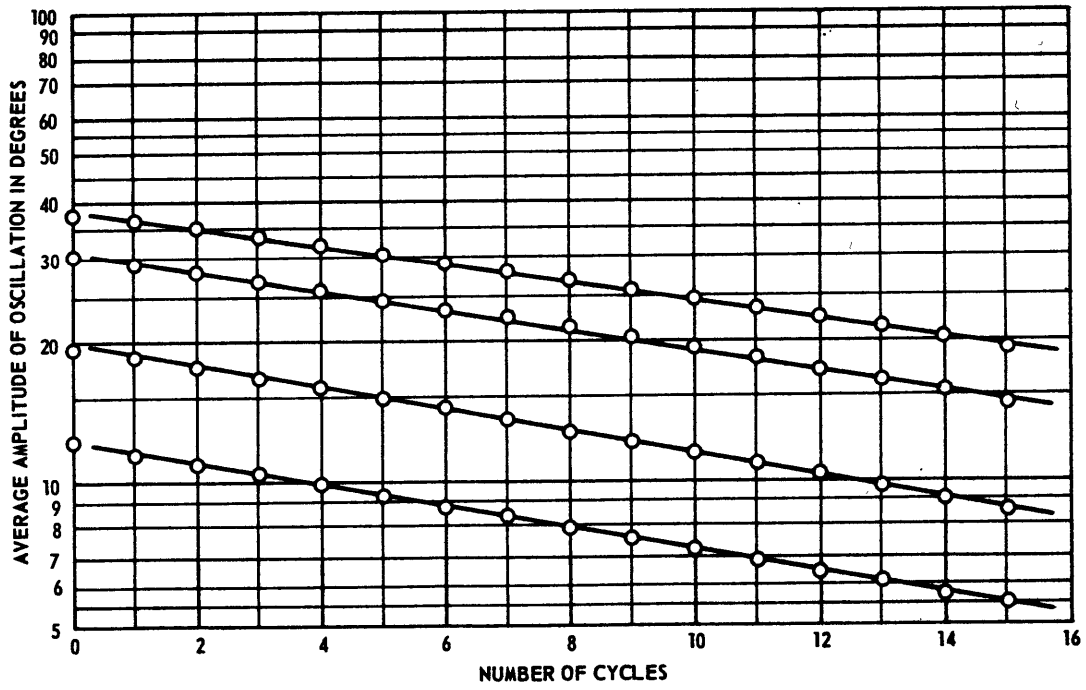

Figure 7 - Amplitude Decay of the 24-Inch-Diameter Bare Cylinder Suspended Vertically in Water

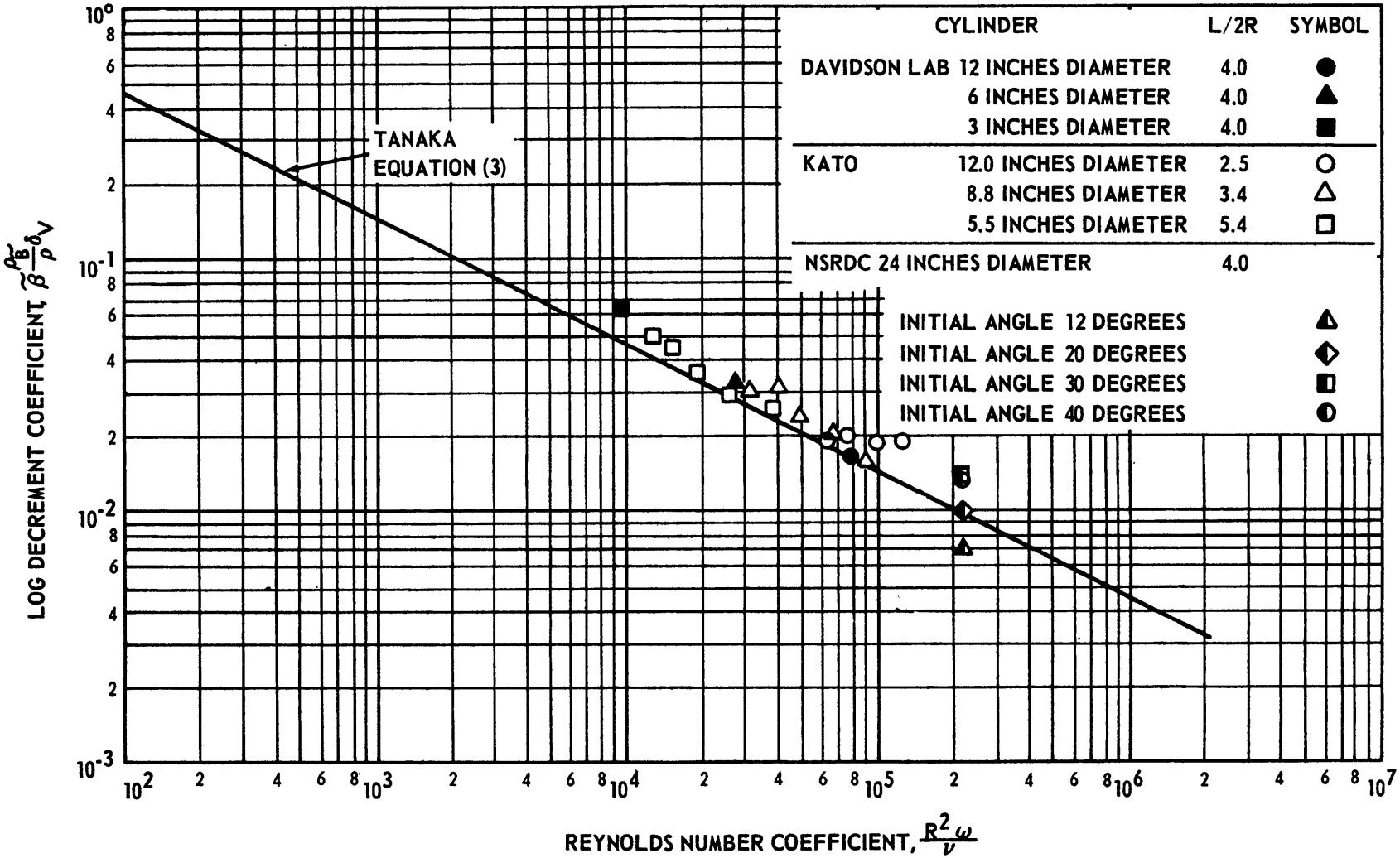

Figure 8 - Comparison Between Theoretical and Experimental Log Decrements for Viscous Roll Damping of Circular Cylinders

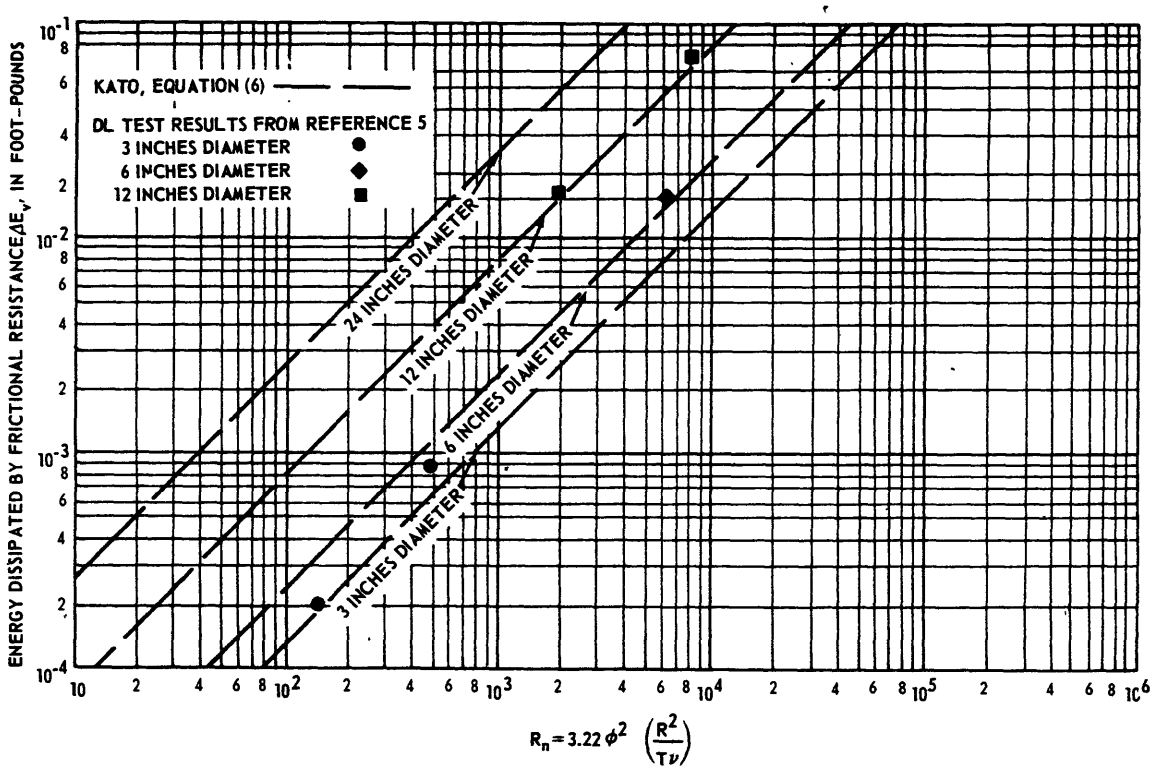

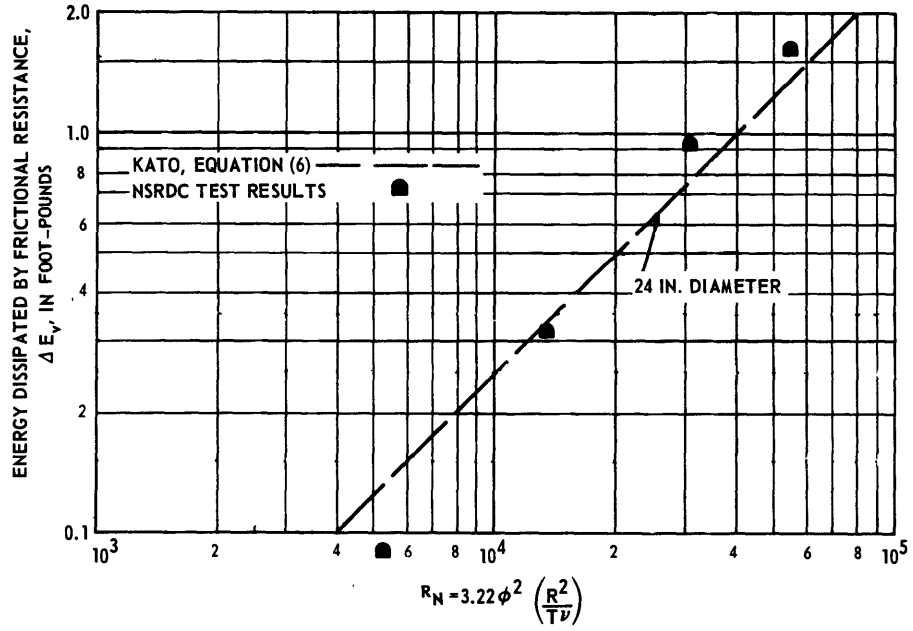

Figure 9 - Comparison Between Predicted and Experimental Energy Dissipation Per Cycle for Viscous Roll Damping of Circular Cylinders, Diameter as Parameter

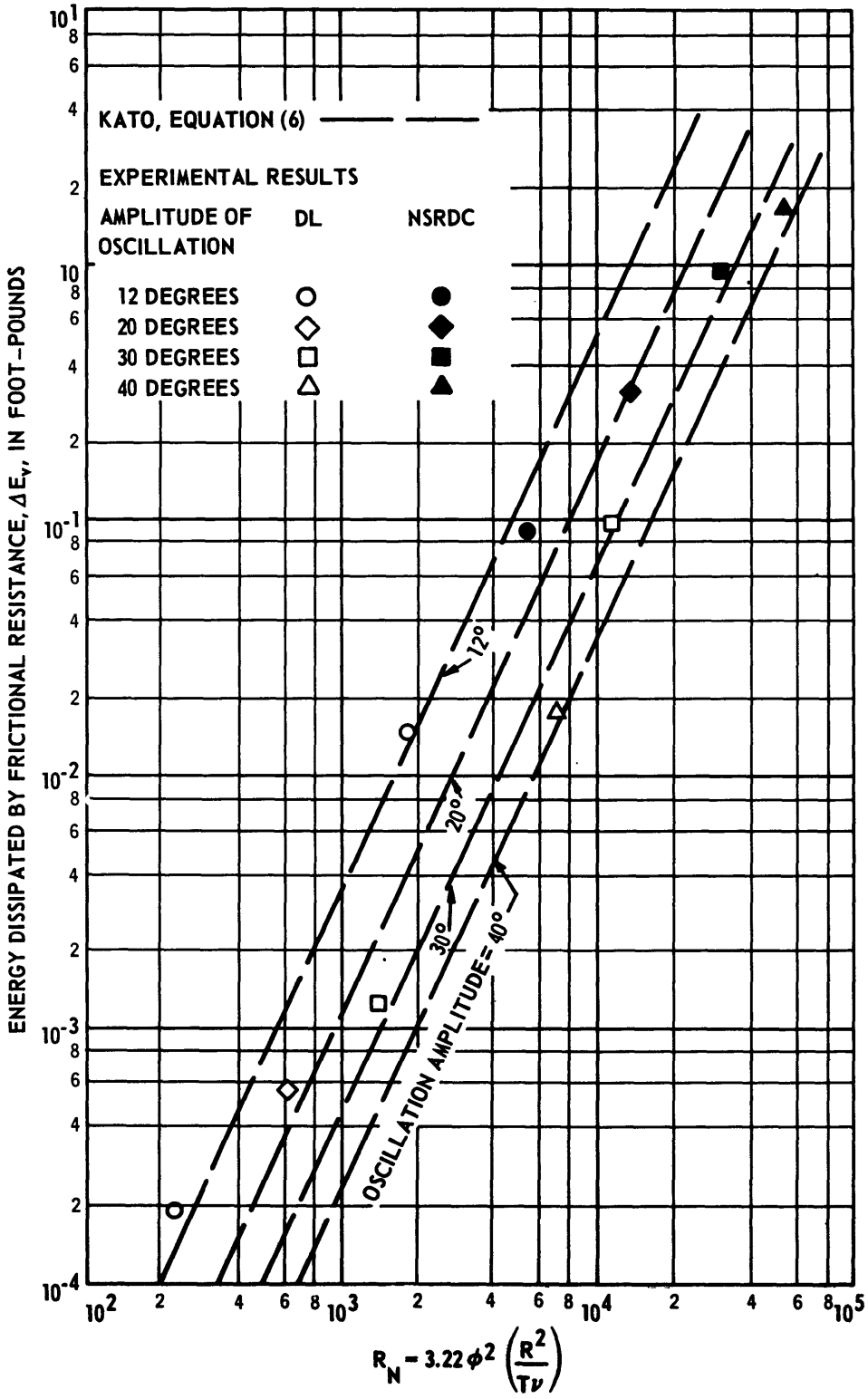

Figure 10 - Comparison Between Predicted and Experimental Energy Dissipation Per Cycle for Viscous Roll Damping of Circular Cylinders, Amplitude of Oscillation as Parameter

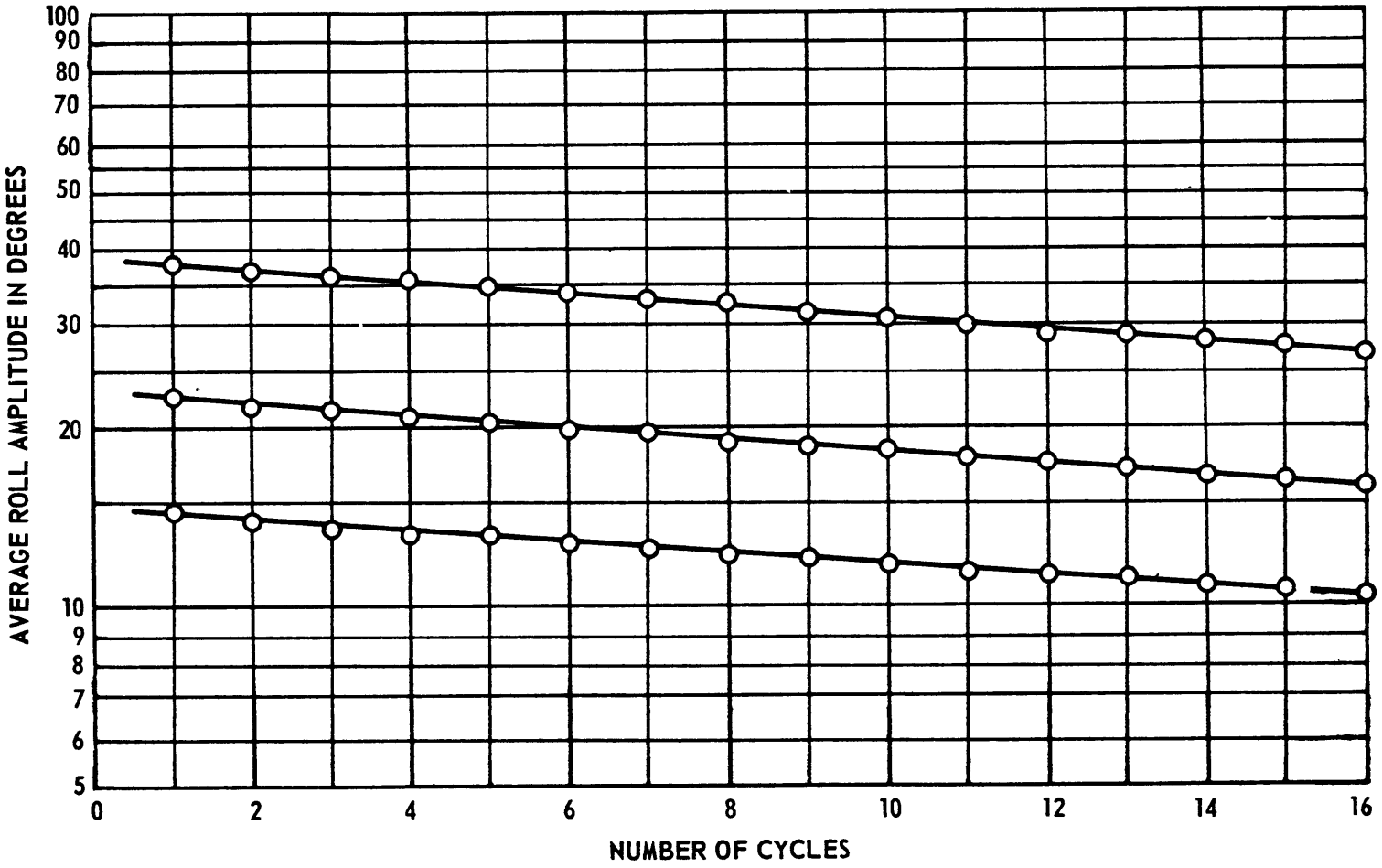

Figure 11 - Amplitude Decay of 24-Inch-Diameter Cylinder Floating Horizontally

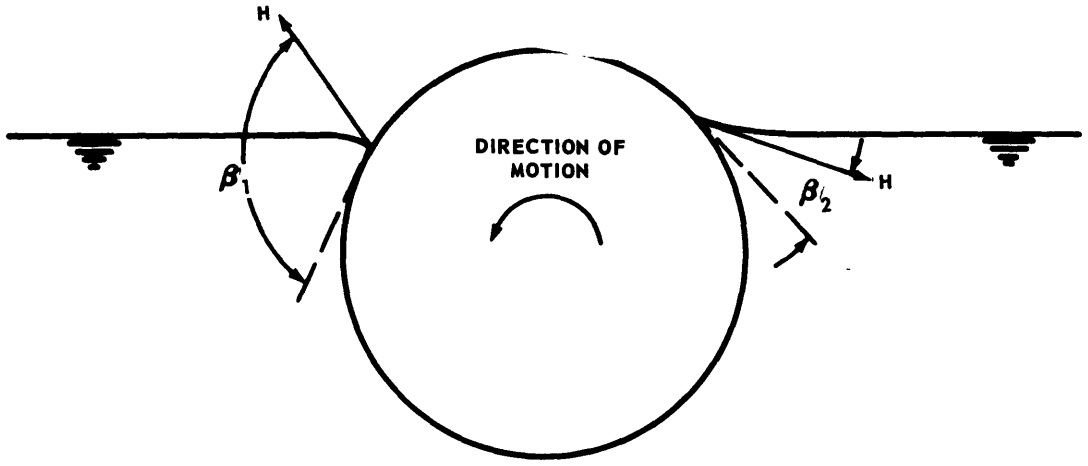

Figure 12a - Surface not Easily Wetted

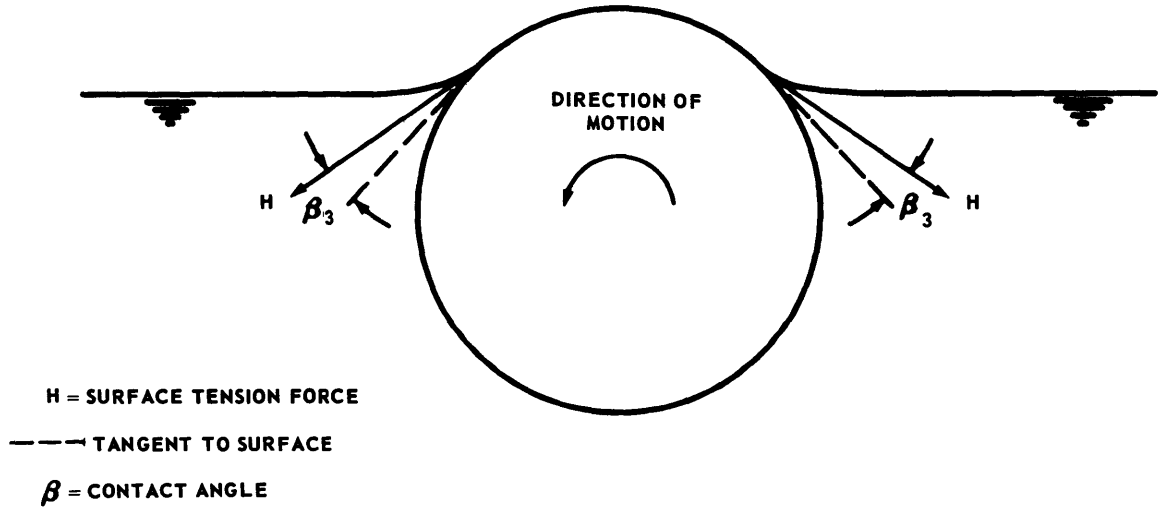

Figure 12b - Surface Easily Wetted

Figure 12 - Effect of Surface Wettability on Surface Tension Damping, After Ueno[3]

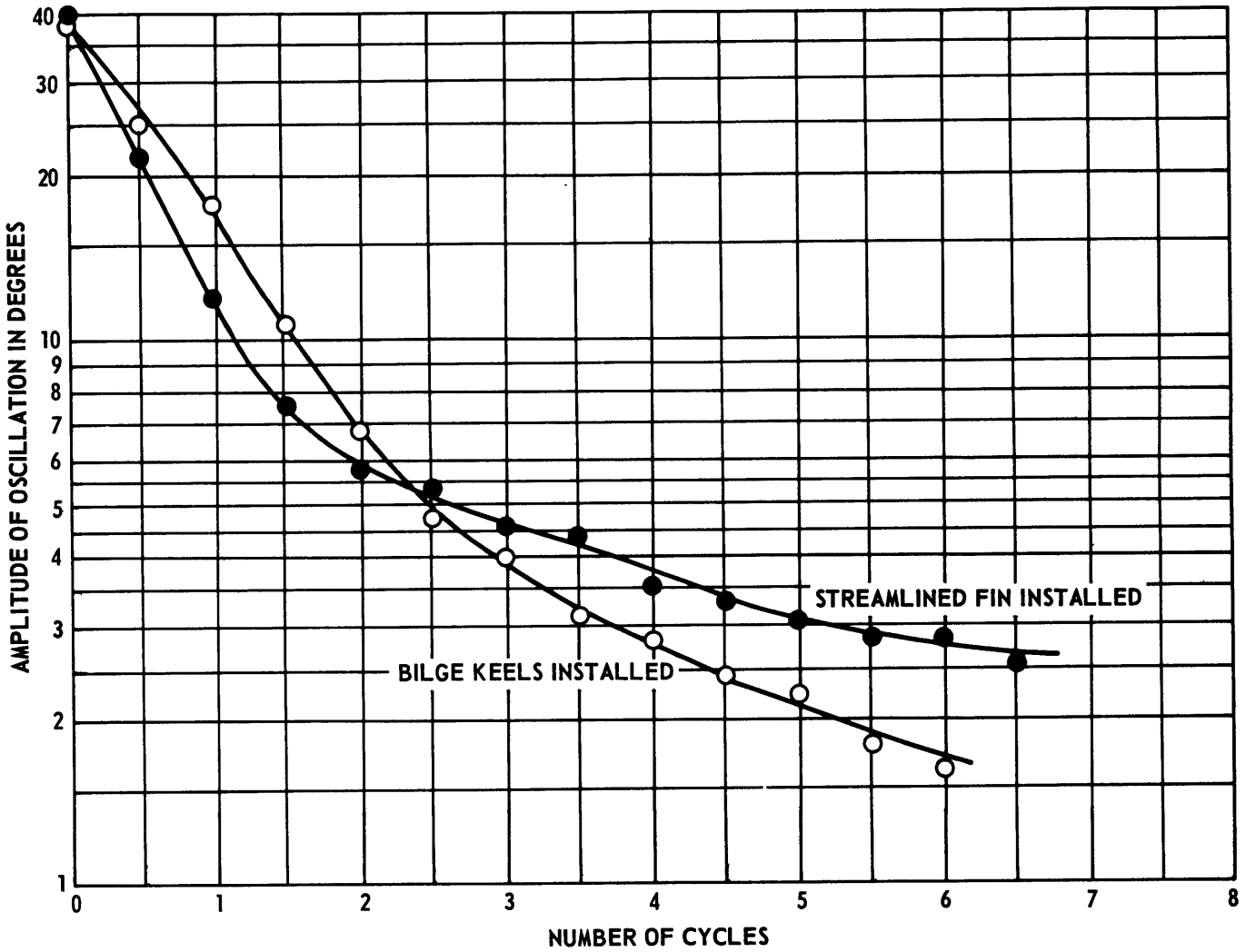

Figure 13 - Amplitude Decay of the 24-Inch-Diameter Appendaged Cylinder Suspended Vertically in Water

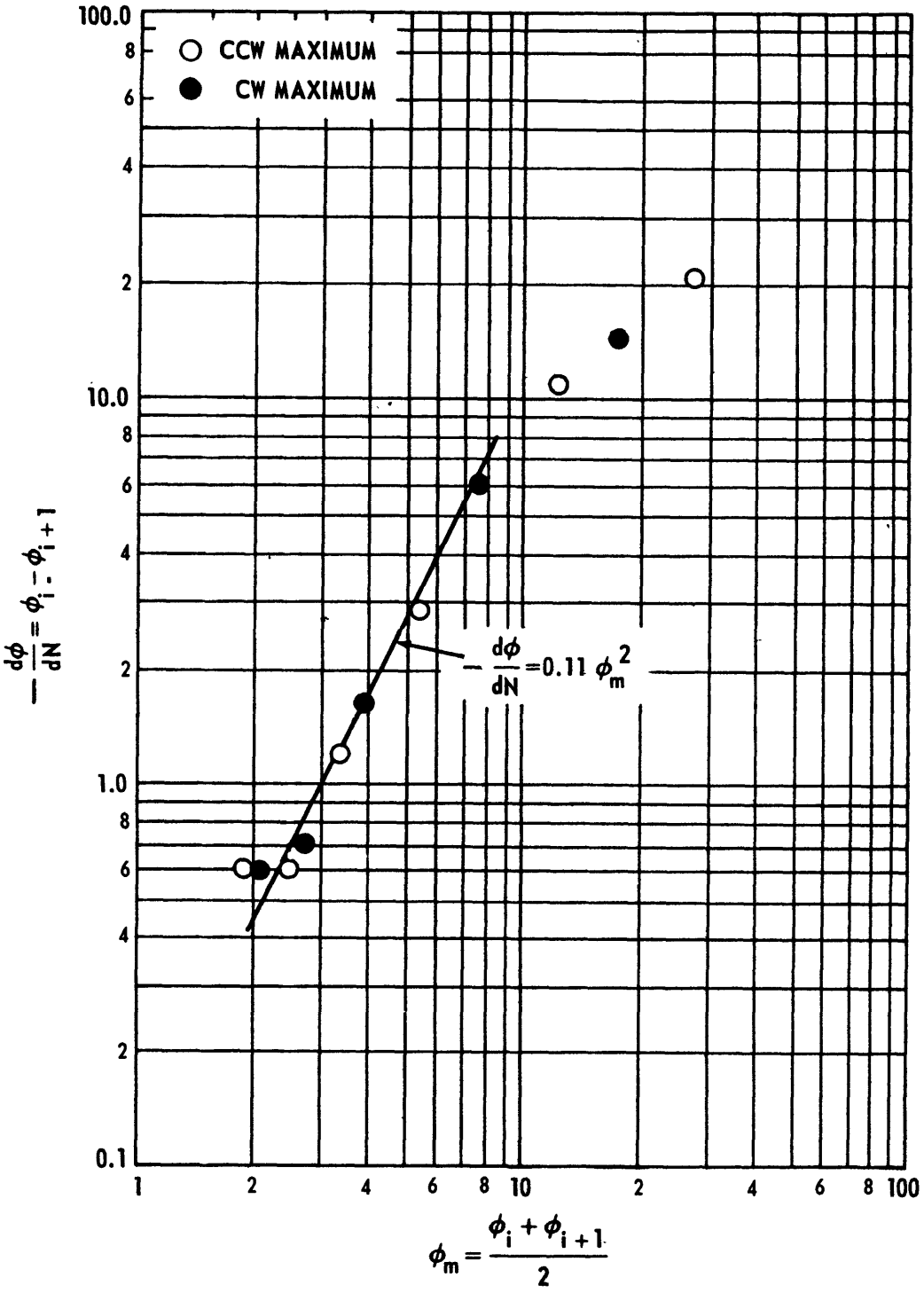

Figure 14 - Decrease in Amplitude Per Period as a Function of the Mean Amplitude, Bilge Keels Installed

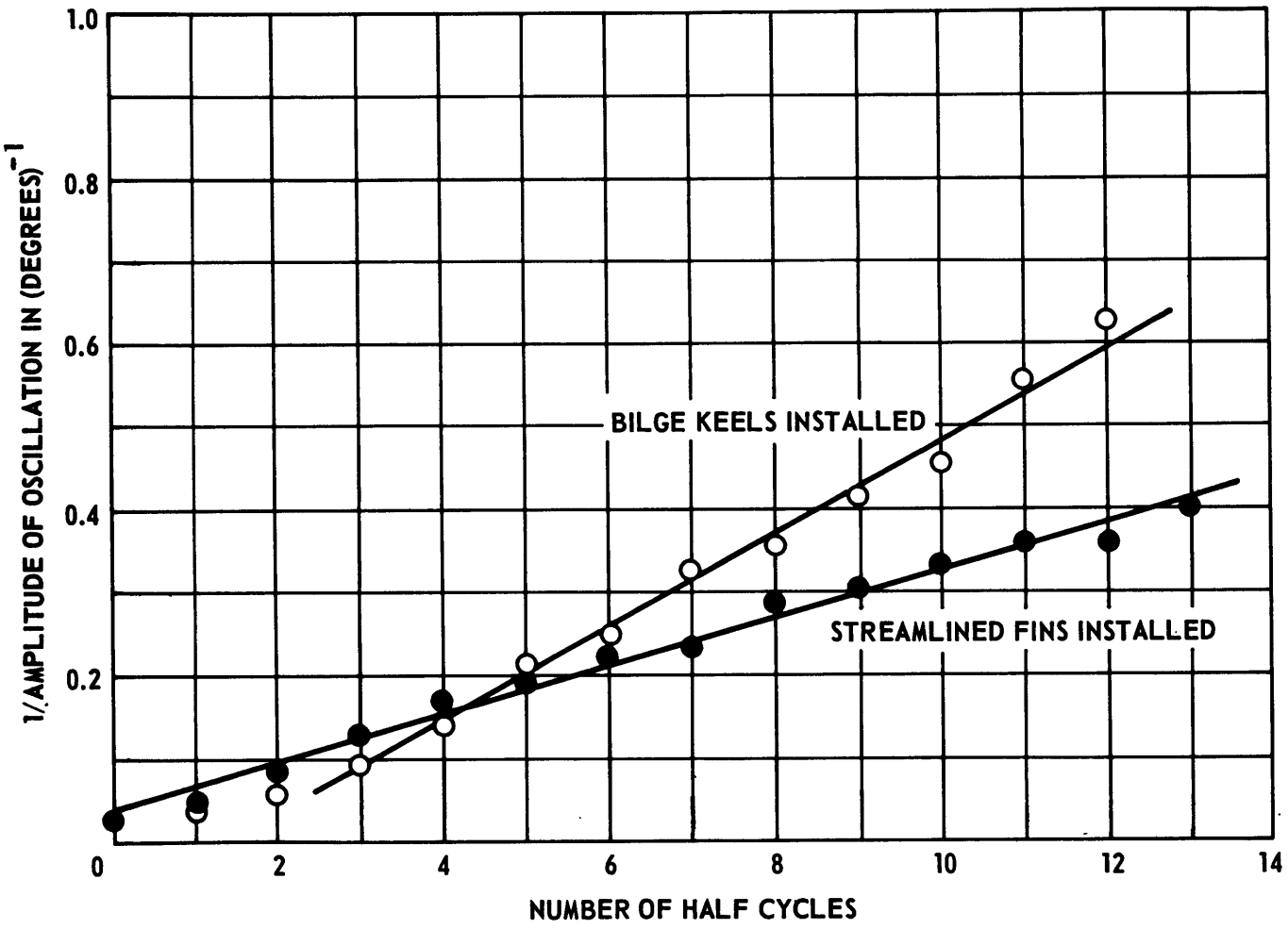

Figure 15 - Typical Plots of Type Utilized to Evaluate Quadratic Damping

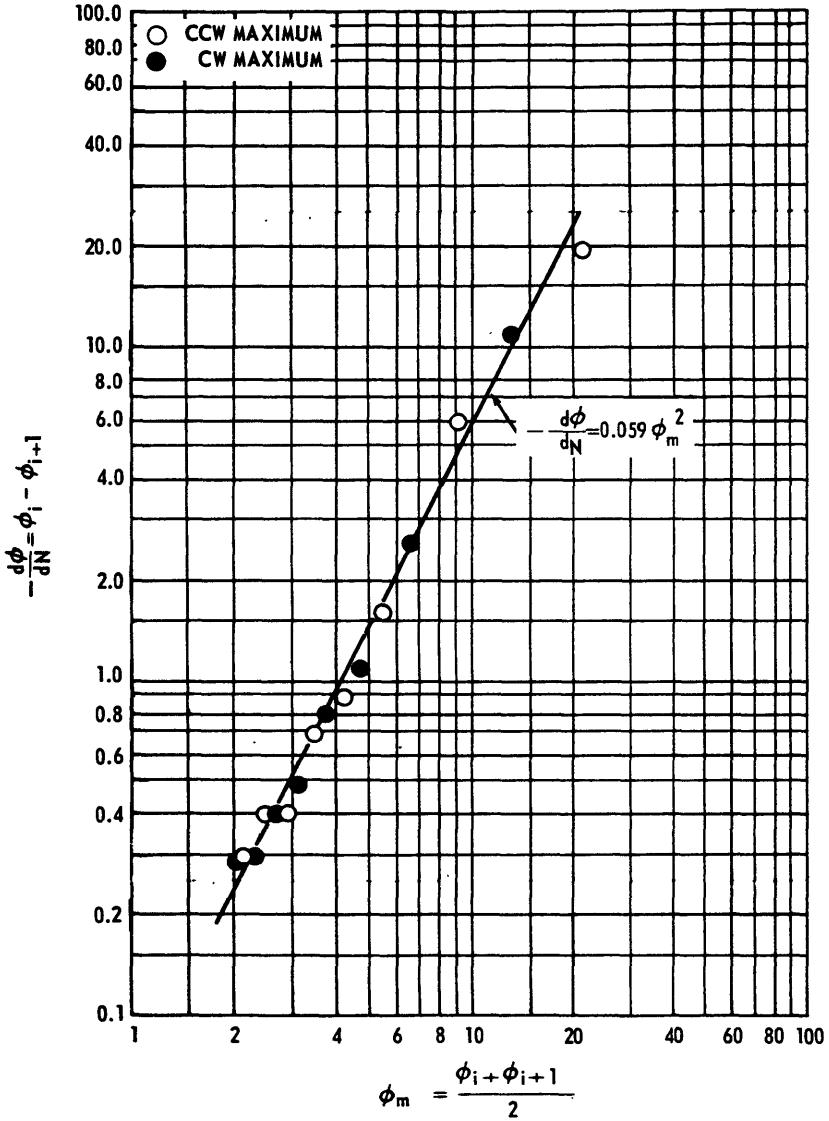

Figure 16 - Decrease in Amplitude Per Period as a Function of the Mean Amplitude, Streamlined Fins Installed

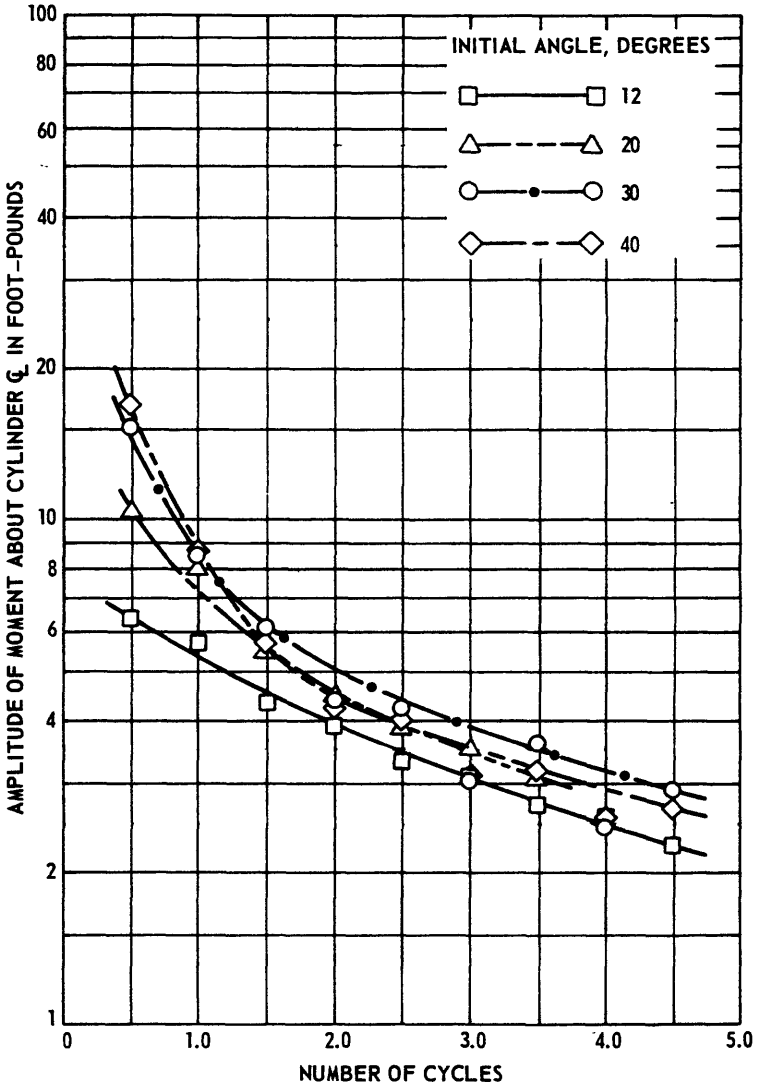

Figure 17 - Moment Produced by One Streamlined Fin

TABLE 1

Dimensions and Dynamic Characteristics of the 24-Inch-Diameter Cylinder

Test Condition	Submerged Length, in.	In Air		Period of Oscillation in Water, T, sec	Restoring Moment Coefficient, in.-lb/deg	$\overline{KG}$, in.
		Weight, lb	Moment of Inertia About ℄, in.-lb-sec^2			
Suspended Vertically						
Bare	96.0	1,848	313.2	2.74	29.1	
Bilge Keels	96.0	1,849	322.0	2.95	29.1	
Streamlined Fin	96.0	1,925	401.0	4.41	29.1	
Floating Horizontally at Submergence of 0.8 x Diameter Bare	96.5	1,353	238.5	2.60	23.9	11.0

TABLE 2

Log Decrements for the Bare Cylinder Suspended Vertically

Initial Angle, deg	δ_B	δ_{V+B}	δ_V
12	0.0394	0.0527	0.0133
20	0.0360	0.0547	0.0187
30	0.0256	0.0509	0.0253
40	0.0218	0.0465	0.0247

TABLE 3

Log Decrements for the Bare Cylinder Floating Horizontally

Initial Angle, deg	$\delta_{V+ST+WM}$
15	0.0219
24	0.0232
40	0.0245

TABLE 4

Energy Loss Per Cycle for the Bare Cylinder Floating Horizontally

Amplitude of Oscillation, deg	$\Delta E_{V+ST+WM}$, ft-lb	ΔE_{V}, ft-lb	ΔE_{ST+WM} ft-lb
12	0.116	0.066	0.050
20	0.315	0.234	0.081
30	0.744	0.695	0.049
40	1.355	1.197	0.158

TABLE 5

Ratio of Components of Energy Loss to Total Energy Loss for the Bare Cylinder Floating Horizontally

Amplitude of Oscillation, deg	$\frac{\Delta E_{V}}{\Delta E_{V+ST+WM}}$	$\frac{\Delta E_{ST+WM}}{\Delta E_{V+ST+WM}}$
	percent	percent
12	56.9	43.1
20	74.3	25.7
30	93.5	6.5
40	88.4	11.6

TABLE 6

Summary of Characteristics and Test Results for Cylinder with Appendages

Appendage	Volume Displaced by Cylinder, ∇, in.^{3}	Appendage Frontal Area, A, in.^{2}	Radius to Centroid of Appendage, $R_{c.a.}$, in.	$\bar{C}_m$ Eq.[13]	C_m Eq.[14]	Period of Oscillation in Water, T, sec	$(I+I_a)/I$ see Eq.[15]
Bilge Keels	43,407	524.2	13.45	0.37	15.0	2.95	1.15
Streamlined Fin	43,407	979.0	19.42	0.39	2.9	4.41	2.05

TABLE 7

Total Energy* Dissipated during the First Cycle of Motion and Its Components, Bilge Keels Installed

Initial Angle, deg	ΔE_{TOTAL} (from Equation [17])	$\Delta E^{\dagger}_{KEELS}$ (from Equation [16])	ΔE_V	$\Delta E_{RESIDUAL}$ $[\Delta E_T-(\Delta E_K+\Delta E_V)]$
20	4.8	4.3	0.2	0.3
30	14.1	11.9	0.6	1.6
40	23.8	20.2	1.0	2.6

*In ft-lb.

†Due to both keels.

TABLE 8

Average Phase between Maximum Clockwise Rotation of Cylinder and Maximum Counter-Clockwise Moment Generated by Streamlined Fins

Initial Angle, deg	Average Phase between Moment and Motion,* ε, deg
12	172
20	172
30	168
40	166

*See definition sketch below.

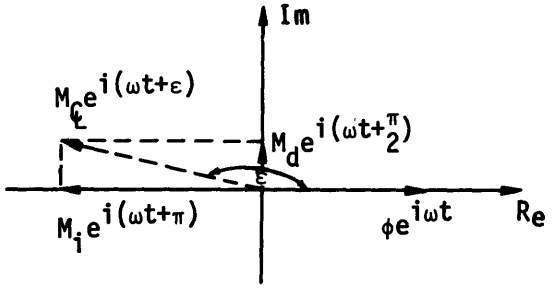

$M_{\mathfrak{C}}$ = amplitude of total moment about cylinder $\mathfrak{C}$

M_d = amplitude of "damping" moment

M_i = amplitude of "acceleration" moment

TABLE 9

Total Energy* Dissipated during One Cycle of Motion** and Its Components, Streamlined Fins Installed

Initial Angle, deg	ΔE_{TOTAL} (from Equation [17])	$\Delta E^{\dagger}_{FINS}$ (from Equation [16])	ΔE_V	$\Delta E_{RESIDUAL}$ $[\Delta E_T-(\Delta E_{FINS}+\Delta E_V)]$
12	0.8	1.3	0	0.5
20	2.4	3.7	0.1	1.4
30	5.6	6.9	0.4	1.7
40	7.9	9.4	0.8	2.3

*In ft-lb.

**Starting at end of first half-cycle.

†Due to both fins.

TABLE 10

Amplitude of Moments Produced by One Fin during First Half-Cycle of Cylinder Rotation in Ft-lb

Initial Angle, deg	M_{ℓ}	M_i*	M_d*	M_d/M_i
12	6.4	6.3	0.9	0.14
20	10.4	10.3	1.4	0.14
30	15.3	14.9	3.2	0.22
40	17.0	16.5	4.1	0.25

*See discussion on page 24

APPENDIX A

NONLINEARITY OF LOG DECREMENT FOR THE BARE CYLINDER

In the body of this report the amplitude decay of the bare cylinder during the first fifteen cycles of oscillation was presented (cf. footnote on page 8), and it appeared to be quite linear for all initial angles. In Figures A1 and A2, the extinction curves are plotted again; this time all the data points obtained from the strip chart records are shown. It can be seen that the slope varies somewhat in the curves for the larger initial angles, especially those for tests in water.

In order to obtain a quantitative measure of the degree of nonlinearity existing, each curve was subdivided into segments eight cycles long, and the log decrement for each quasi-linear region was computed. The results are given in Table A1 which shows that δ_V for the smaller initial angles has a tendency to decrease as the mean angle for a segment decreases (higher region number), and that δ_V for the larger initial angles tends to increase as the mean angle decreases. Although for small damping the experimental errors make it difficult to determine trends, it is evident that the log decrements are not constant, and therefore the existence of slightly nonlinear damping for the bare cylinder is implied.

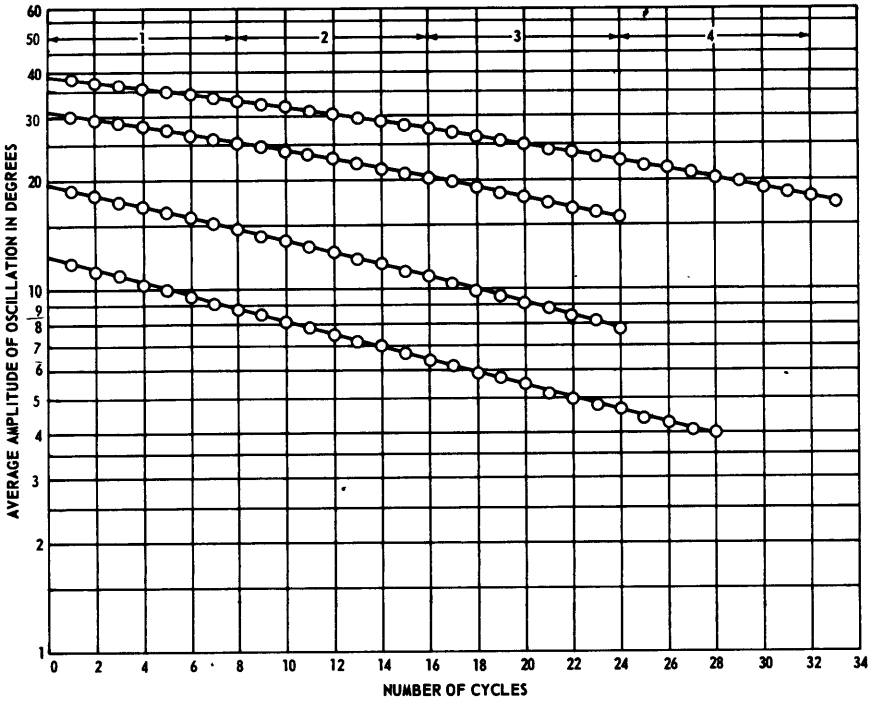

Figure A1 - Amplitude Decay of the 24-Inch-Diameter Bare Cylinder Suspended Vertically in Air, for Examination of Nonlinearity

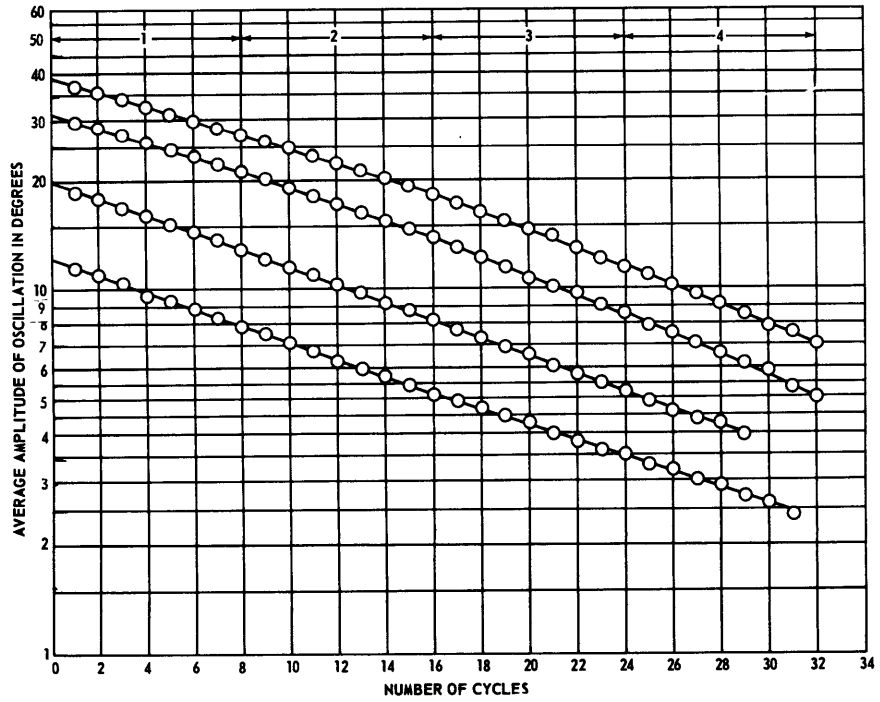

Figure A2 - Amplitude Decay of the 24-Inch-Diameter Bare Cylinder Suspended Vertically in Water, for Examination of Nonlinearity

TABLE A1

Log Decrements for the Bare Cylinder Suspended Vertically, for Examination of Nonlinearity

Region	Initial Angle, degrees											
	12			20			30			40		
	δ_B	δ_{V+B}	δ_V	δ_B	δ_{V+B}	δ_V	δ_B	δ_{V+B}	δ_V	δ_B	δ_{V+B}	δ_V
1	0.0428	0.0543	0.0115	0.0351	0.0545	0.0194	0.0235	0.0470	0.0235	0.0201	0.0449	0.0248
2	0.0388	0.0547	0.0159	0.0382	0.0556	0.0174	0.0267	0.0527	0.0260	0.0230	0.0486	0.0256
3	0.0393	0.0475	0.0082	0.0406	0.0562	0.0156	0.0319	0.0622	0.0303	0.0254	0.0600	0.0346
4	---	0.0497	---	---	0.0528	---	---	0.0677	---	0.0276	0.0642	0.0366

BLANK

APPENDIX B

THEORETICAL CALCULATION OF CYLINDER MOTION AND ENERGY LOSS

The angular motion of the cylinder with appendages, $\phi(t)$, can be computed from the solution of Equation [10] in the body of this report. The solution was given as

$$\phi(t) = a(t) \cos \omega t \qquad [11]$$

where

$$\frac{1}{a(t)} = \frac{1}{a_o} + \frac{4\, b\, \omega^2}{3k}\, n \qquad [12]$$

All of the constants in Equation [12] can be obtained from results presented in this paper. Computations of $\phi(t)$ were carried out on the IBM 7090 digital computer for the bilge keel and fin configurations. A comparison of the theoretical and empirical (as read from the strip chart record) time histories for one cycle with fins installed is made in Figure B1. The agreement is good; however, the theoretical curve damps out somewhat more slowly than the experimentally obtained curve.

Analytical calculations were also made of the total energy loss per cycle by means of the following equation

$$\tilde{\Delta E}_{TOTAL} = \oint b\, \dot{\phi}^2\, |\dot{\phi}|\, dt = \oint I_{virtual}\, \ddot{\phi}\, \dot{\phi}\, dt + \oint k\, \phi\, \dot{\phi}\, dt \qquad [B1]$$

The integration was always started at a time of maximum displacement and carried on for one period so that the angular velocity was zero at both end points. As a result, the work due to the inertial term which is represented by the difference in kinetic energy at the end points [i.e., $1/2\ I_{virtual}\ (\dot{\phi}_2^2 - \dot{\phi}_1^2)$] should be zero. The computer outputs showed it to be extremely small compared to the other terms, so that the energy represented by the damping term was almost equal to that associated with the restoring moment term. The latter two were averaged, and in Tables B1 and B2 the results are compared to ΔE_{TOTAL} as obtained from the strip chart records and Equation [17]. It should be pointed out that the b-value inserted in Equation [B1] for the bilge keel configuration was obtained by

fairing a straight line through the first three points of the $1/\phi$ versus n plot. This was done because the slope for these initial transient oscillations was generally different from that for the subsequent cycles. The curves for the fin-equipped cylinder did not exhibit such a radical change in slope during the first few cycles so that b was essentially constant for all values of n. The values of ΔE_{TOTAL} in Table B2 were derived after inserting the actual initial angle into the solution of the equation of motion. They do not agree exceptionally well with the true energy loss, especially for large initial angles. If, however, the amplitude at the end of the first half-cycle were read from the strip chart* and utilized as the initial condition in Equation [11], the correspondence would be much better. For example, $\tilde{\Delta E}_{TOTAL}$ for ϕ_o = 40 deg would change from 5.4 to 7.4 ft-lb.

*Of course, one would not usually be performing theoretical computations of ΔE_{TOTAL} if $\phi(t)$ were available from experiments.

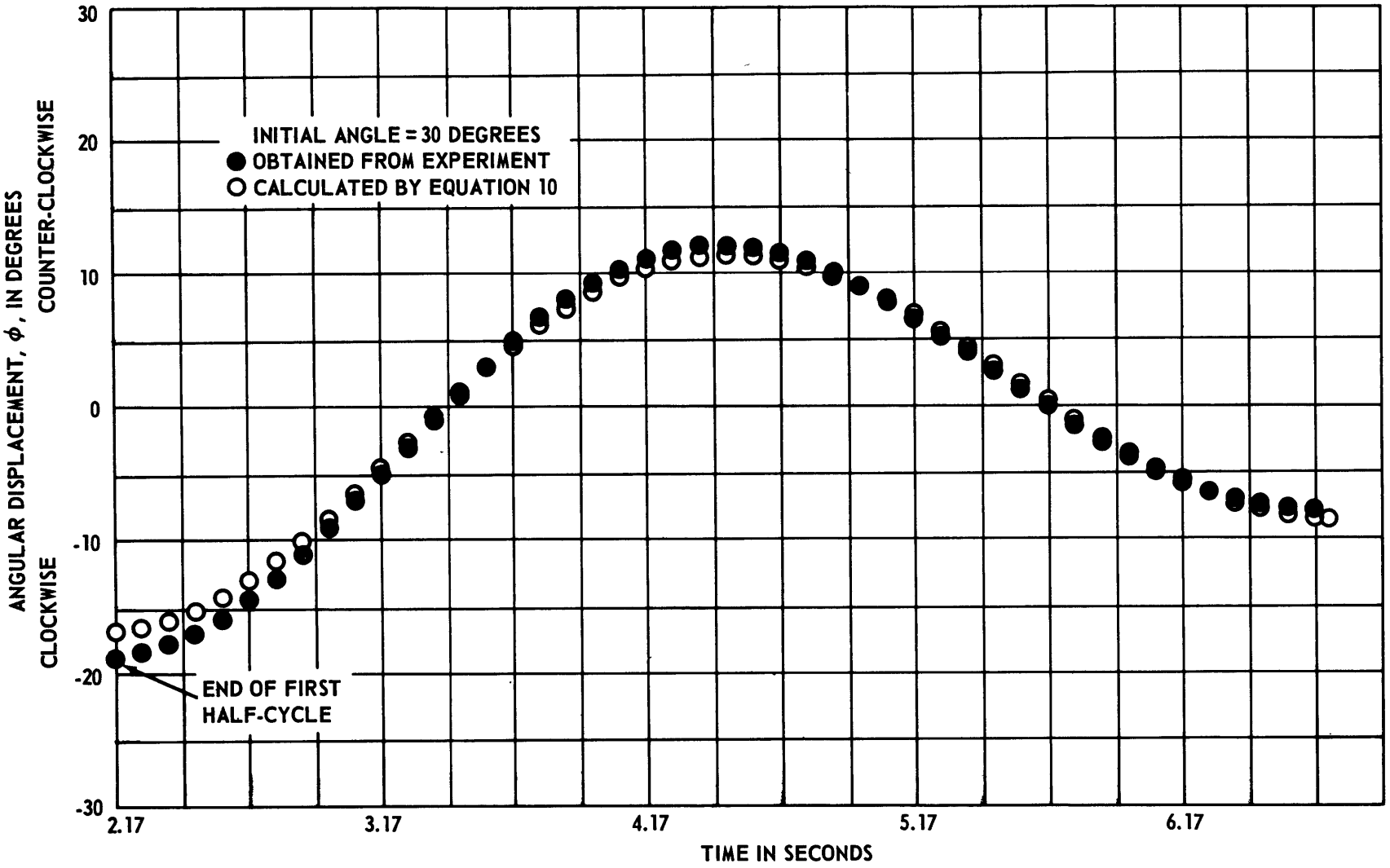

Figure B1 - Comparison Between Actual and Computed Time Histories of Motion for Cylinder with Streamlined Fins Installed

TABLE B1

Comparison between Actual and Computed Total Energy* Loss Per Cycle,† Bilge Keels Installed

Initial Angle, deg	ΔE_{TOTAL} [Experiment]	$\widetilde{\Delta E}_{TOTAL}$ [Theory]	Percent Difference
20	4.8	4.6	4.2
30	14.1	13.9	1.4
40	23.8	22.0	7.6

*In ft-lb.

†First cycle.

TABLE B2

Comparison between Actual and Computed Total Energy* Loss Per Cycle,† Streamlined Fins Installed

Initial Angle, deg	ΔE_{TOTAL} [Experiment]	ΔE_{TOTAL} [Theory]	Percent Difference
12	0.8	0.7	12.5
20	2.4	2.0	16.7
30	5.6	4.3	23.2
40	7.9	5.4	31.6

*In ft-lb.

†Started at end of first half-cycle.

REFERENCES

1. Kato, Hirosi, "On the Nature of Resistance to Rolling of Ships and the Law of Comparison," J. of Zosen Kiokai, Vol. 66 (1940). In Japanese

2. Kato, Hirosi, "On the Frictional Resistance to the Rolling of Ships," J. of Zosen Kiokai, Vol. 102 (1957). In Japanese

3. Ueno, Keizo, "Influence of the Surface Tension of the Surrounding Water Upon the Free Rolling of Model Ships," Memoirs of the Faculty of Engineering, Kyushu University, Vol. XII, No. 1 (1950).

4. Ochi, Kazuo M., "Notes on Roll Behavior of SSBN - Class Submarines," David Taylor Model Basin Preliminary Report (Sep 1963). CONFIDENTIAL

5. Mercier, John A., "Scale Effect on Roll-Damping Forces at Zero Forward Speed," Davidson Laboratory Report 1057 (Feb 1965).

6. Mercier, John A., "Effect of Proportions on Roll-Damping of Oscillating Cylinders Due to Viscous Shear Stress," Davidson Laboratory Letter Report 1088 (Jul 1965).

7. Karp, S. and Kotik, J., "Wavemaking Due to Tangential Forced Motion in a Viscous Fluid," Preliminary report of research done by Technical Research Group, Melville, N.Y., for U.S. Navy, under contract Nonr-3611 (00) (Sep 1963).

8. Kestin, Joseph and Persen, Leif, N., "Slow Oscillations of an Infinite Plate and an Infinite Disk in a Viscous Fluid," Brown University Report AF-891/1 (Jun 1954).

9. Thomson, W.T., "Mechanical Vibrations," Prentice-Hall, Inc. Publishers (Jun 1963).

10. Cummins, W.E., "The Impulse Response Function and Ship Motions," Shiffstechnik, Vol. 9, No. 47 (Jun 1962).

11. Tanaka, I., "Viscous Damping of Rotational Oscillations of a Cylinder," Davidson Laboratory Note 719 (Jun 1964).

12. McLeod, W.C. and Hsieh, Tsuying, "Experimental Investigation of Ursell's Theory of Wavemaking by a Rolling Cylinder," Schiffstechnik, Bd. 10, Heft 50 (1963).

13. Gawn, R.W.L., "Rolling Experiments with Ships and Models in Still Water," Trans. Inst. Naval Arch., Vol. 82 (1940).

14. Brown, P. Ward, "The Effect of Configuration on the Drag of Oscillating Damping Plates," Davidson Laboratory Report 1021 (May 1964).

15. Minorsky, N., "Nonlinear Oscillations," Published by D. Van Nostrand Co., Inc., Princeton, N.J. (1962).

16. Keulegan, G.H. and Carpenter, L.H., "Forces on Cylinders and Plates in an Oscillating Fluid," Journal of Research of the National Bureau of Standards, Vol. 60, No. 5 (May 1958).

17. Ridjanovic, M., "Drag Coefficients of Flat Plates Oscillating Normally to Their Planes," Schiffstechnik, Vol. 9, No. 45 (Jan 1962).

INITIAL DISTRIBUTION

Copies

- 3 NAVSHIPSYSCOM
  - 2 SHIPS 2052
  - 1 SHIPS 0341
- 6 NAVSEC
  - 2 SEC 6110
  - 2 SEC 6122
  - 2 SEC 6136
- 2 CHONR
  - 1 Code 438
  - 1 Code 466
- 1 ONR, New York
- 1 ONR, Pasadena
- 1 ONR, Chicago
- 1 ONR, Boston
- 1 ONR, London
- 1 NMDL
- 1 NAVUWRES
- 1 NOL
- 1 CDR, NUWC
- 1 CDR, NWC
- 1 NRL
- 2 D.L., SIT
  - 1 John A. Mercier
  - 1 Dr. J. Breslin
- 1 DIR, DEF R&E
- 1 Dir, Exptl Nav Tank
  Univ of Mich, Ann Arbor
- 1 Dir, Inst for Fluid Dyn & Appl Math,
  Univ of Md
- 1 Dir, Scripps Inst of Ocean, Univ of Calif
- 1 Dir, WHOI, Woods Hole
- 1 Dir, ORL, Penn State
- 1 CO, USNROTC & NAVAMINU, MIT

Copies

- 1 James Forrestal Res Ctr, Princeton
  Univ, Princeton
  Attn: Mr. Maurice H. Smith, Asst to Dir
- 2 SUPSHIP, Quincy, Mass
- 2 NNS & DD Co
  - 1 Asst Nav Arch
  - 1 Dir, Hydra Lab
- 20 CDR, DDC
- 1 MARAD (Res & Dev Sec)
- 1 Catholic Univ, Applied Mechanics Div
  School of Eng & Arch
- 1 Prof. J.R. Paulling
  College of Eng, University of Calif, Berkeley
- 2 NYU, Dept of Oceanography & Meteorology
  - 1 Dr. W.J. Pierson, Jr.
  - 1 Mr. R. Johnson
- 2 DIR, SPO
- 1 General Dynamics Corp, Electric Boat Div
- 1 Oceanics, Inc., Technical Industrial Park
- 1 Westinghouse Electric Corp, Annapolis, Md.
  Attn: Mr. M.S. Macovsky
- 1 SNAME
  Attn: Panel H-7
- 1 Dir, Natl BuStand
- 1 Dir, APL/JHU
- 1 Dir, Fluid Mech Lab, Columbia Univ,
  New York, N.Y.
- 1 Dir, Hydra Lab, Univ of Colorado
  Boulder, Colorado
- 1 Dir, Hydra Res Lab, Univ of Conn,
  Storrs, Conn.
- 1 Dir, Robinson Hydra Lab, Ohio St Univ,
  Columbus, Ohio
- 1 Dir, Hydra Lab, Penn State Univ,
  University Park, Pa.

Copies

1 Dir, Hydra Lab, Univ of Wisconsin

1 Dir, Hydra Lab, Univ of Washington

1 SAFHL/Univ of Minn

1 Dir of Res, The Tech Inst, Northwestern Univ
Evanston, Ill.

2 NPTNWS SHIPBLDG & DD CO

1 Dr. M.L. Albertson, Head of Fluid Mech Res,
Dept of Civil Engr, Colorado St Univ,
Fort Collins, Colo

1 MIT, Dept of NA&ME

1 Lockheed Missiles & Space Co
Sunnyvale, Calif

1 MIT Hayden Lib
Ser & Doc Div
Cambridge, Mass

2 President, Webb Inst of Nav Arch
Glen Cove, Long Island, N.Y.
1 Prof. Nevitt

1 Dir, Iowa Inst of Hydra Res
St Univ of Iowa, Iowa City, Iowa

1 Editor, Bibliography of Tech Reports
Office of Tech Services
U.S. Dept of Commerce
Washington 25, D.C.

UNCLASSIFIED

Security Classification

DOCUMENT CONTROL DATA - R & D

(Security classification of title, body of abstract and indexing annotation must be entered when the overall report is classified)

1. ORIGINATING ACTIVITY *(Corporate author)*

Naval Ship Research and Development Center
Washington, D.C. 20007

2a. REPORT SECURITY CLASSIFICATION

UNCLASSIFIED

2b. GROUP

3. REPORT TITLE

ROLL DAMPING OF CIRCULAR CYLINDERS WITH AND WITHOUT APPENDAGES

4. DESCRIPTIVE NOTES *(Type of report and inclusive dates)*

5. AUTHOR(S) *(First name, middle initial, last name)*

Alvin Gersten

6. REPORT DATE	7a. TOTAL NO. OF PAGES	7b. NO. OF REFS
October 1969	64	17

8a. CONTRACT OR GRANT NO.	9a. ORIGINATOR'S REPORT NUMBER(S)
b. PROJECT NO. S-F013 02 03 Task 1711	2621
c.	9b. OTHER REPORT NO(S) *(Any other numbers that may be assigned this report)*
d.	

10. DISTRIBUTION STATEMENT

This document has been approved for public release and sale; its distribution is unlimited.

11. SUPPLEMENTARY NOTES	12. SPONSORING MILITARY ACTIVITY
	Naval Ship Engineering Center

13. ABSTRACT

A research program established to provide scaling laws for roll damping involves testing five circular cylinders ranging from 3 in. to 4 ft in diameter. This report presents the results of experiments conducted on the fourth cylinder in the series, which has a 2-ft diameter and which, like those tested before it, was oscillated freely at zero forward speed. The experiments were carried out with the cylinder suspended vertically in the water both with and without appendages, and with the bare cylinder floating horizontally. In this way, the various components of damping can be isolated. Log decrements and energy loss per cycle for the bare cylinder, as well as energy loss and moment coefficients for the appendaged cylinder, are presented herein.

The results obtained thus far in the program indicate that reasonably good methods of predicting the viscous damping of different size models are available. At the conclusion of experiments with the largest cylinder in the series, sufficient information should be available for the development of an empirical equation for eddy-making damping; however, since the waves generated by the cylinder are extremely small, and therefore difficult to measure, it may not be possible to separate the contribution of wave-making damping from that of surface tension by means of the test methods presently employed.

DD FORM 1 NOV 68 1473 (PAGE 1)

S/N 0101-807-6801

UNCLASSIFIED

Security Classification

14. KEY WORDS	LINK A		LINK B		LINK C	
	ROLE	WT	ROLE	WT	ROLE	WT
Roll damping						
Rolling Cylinders						
Viscous damping						
Eddy-making damping						
Surface tension damping						
Wavemaking damping						

Naval Ship R&D Center. Report 2621.
ROLL DAMPING OF CIRCULAR CYLINDERS WITH AND WITHOUT APPENDAGES, by Alvin Gersten. Oct 1969. vi, 58p. illus., refs. UNCLASSIFIED

A research program established to provide scaling laws for roll damping involves testing five circular cylinders ranging from 3 in. to 4 ft in diameter. This report presents the results of experiments conducted on the fourth cylinder in the series, which has a 2-ft diameter and which, like those tested before it, was oscillated freely at zero forward speed. The experiments were carried out with the cylinder suspended vertically in the water both with and without appendages, and with the bare cylinder floating horizontally. In this way, the various components of damping can be isolated. Log decrements and energy loss per cycle for the bare cylinder, as well as energy loss and moment coefficients for the appendaged cylinder, are presented herein.

The results obtained thus far in the program indicate that reasonably good methods of predicting the viscous damping of different size models are available. At the conclusion of experiments with the largest cylinder in the series, sufficient information should be available for the development of an empirical equation for eddy-making damping; however, since the waves generated by the cylinder are extremely small, and therefore difficult to measure, it may not be possible to separate the contribution of wave-making damping from that of surface tension by means of the test methods presently employed.

1. Submarines--Roll--Damping--Model tests
2. Submarines--Roll--Damping--Scaling effects
3. Submarines--Appendages--Damping--Model tests--Scaling effects
4. Damping--Wave-making--Model tests--Scaling effects
5. Damping--Eddy-making--Model tests Scaling effects

I. Gersten, Alvin
II. Title: Roll damping of circular cylinders

Naval Ship R&D Center. Report 2621.
ROLL DAMPING OF CIRCULAR CYLINDERS WITH AND WITHOUT APPENDAGES, by Alvin Gersten. Oct 1969. vi, 58p. illus., refs. UNCLASSIFIED

A research program established to provide scaling laws for roll damping involves testing five circular cylinders ranging from 3 in. to 4 ft in diameter. This report presents the results of experiments conducted on the fourth cylinder in the series, which has a 2-ft diameter and which, like those tested before it, was oscillated freely at zero forward speed. The experiments were carried out with the cylinder suspended vertically in the water both with and without appendages, and with the bare cylinder floating horizontally. In this way, the various components of damping can be isolated. Log decrements and energy loss per cycle for the bare cylinder, as well as energy loss and moment coefficients for the appendaged cylinder, are presented herein.

The results obtained thus far in the program indicate that reasonably good methods of predicting the viscous damping of different size models are available. At the conclusion of experiments with the largest cylinder in the series, sufficient information should be available for the development of an empirical equation for eddy-making damping; however, since the waves generated by the cylinder are extremely small, and therefore difficult to measure, it may not be possible to separate the contribution of wave-making damping from that of surface tension by means of the test methods presently employed.

1. Submarines--Roll--Damping--Model tests
2. Submarines--Roll--Damping--Scaling effects
3. Submarines--Appendages--Damping--Model tests--Scaling effects
4. Damping--Wave-making--Model tests--Scaling effects
5. Damping--Eddy-making--Model tests Scaling effects

I. Gersten, Alvin
II. Title: Roll damping of circular cylinders

Naval Ship R&D Center. Report 2621.
ROLL DAMPING OF CIRCULAR CYLINDERS WITH AND WITHOUT APPENDAGES, by Alvin Gersten. Oct 1969. vi, 58p. illus., refs. UNCLASSIFIED

A research program established to provide scaling laws for roll damping involves testing five circular cylinders ranging from 3 in. to 4 ft in diameter. This report presents the results of experiments conducted on the fourth cylinder in the series, which has a 2-ft diameter and which, like those tested before it, was oscillated freely at zero forward speed. The experiments were carried out with the cylinder suspended vertically in the water both with and without appendages, and with the bare cylinder floating horizontally. In this way, the various components of damping can be isolated. Log decrements and energy loss per cycle for the bare cylinder, as well as energy loss and moment coefficients for the appendaged cylinder, are presented herein.

The results obtained thus far in the program indicate that reasonably good methods of predicting the viscous damping of different size models are available. At the conclusion of experiments with the largest cylinder in the series, sufficient information should be available for the development of an empirical equation for eddy-making damping; however, since the waves generated by the cylinder are extremely small, and therefore difficult to measure, it may not be possible to separate the contribution of wave-making damping from that of surface tension by means of the test methods presently employed.

1. Submarines--Roll--Damping--Model tests
2. Submarines--Roll--Damping--Scaling effects
3. Submarines--Appendages--Damping--Model tests--Scaling effects
4. Damping--Wave-making--Model tests--Scaling effects
5. Damping--Eddy-making--Model tests Scaling effects

I. Gersten, Alvin
II. Title: Roll damping of circular cylinders

Naval Ship R&D Center. Report 2621.
ROLL DAMPING OF CIRCULAR CYLINDERS WITH AND WITHOUT APPENDAGES, by Alvin Gersten. Oct 1969. vi, 58p. illus., refs. UNCLASSIFIED

A research program established to provide scaling laws for roll damping involves testing five circular cylinders ranging from 3 in. to 4 ft in diameter. This report presents the results of experiments conducted on the fourth cylinder in the series, which has a 2-ft diameter and which, like those tested before it, was oscillated freely at zero forward speed. The experiments were carried out with the cylinder suspended vertically in the water both with and without appendages, and with the bare cylinder floating horizontally. In this way, the various components of damping can be isolated. Log decrements and energy loss per cycle for the bare cylinder, as well as energy loss and moment coefficients for the appendaged cylinder, are presented herein.

The results obtained thus far in the program indicate that reasonably good methods of predicting the viscous damping of different size models are available. At the conclusion of experiments with the largest cylinder in the series, sufficient information should be available for the development of an empirical equation for eddy-making damping; however, since the waves generated by the cylinder are extremely small, and therefore difficult to measure, it may not be possible to separate the contribution of wave-making damping from that of surface tension by means of the test methods presently employed.

1. Submarines--Roll--Damping--Model tests
2. Submarines--Roll--Damping--Scaling effects
3. Submarines--Appendages--Damping--Model tests--Scaling effects
4. Damping--Wave-making--Model tests--Scaling effects
5. Damping--Eddy-making--Model tests Scaling effects

I. Gersten, Alvin
II. Title: Roll damping of circular cylinders